Acta Pharmaceutica Sinica B xxxx;xxx(xxx):xxx

Chinese Pharmaceutical Association
Institute of Materia Medica, Chinese Academy of Medical Sciences

Acta Pharmaceutica Sinica B

www.elsevier.com/locate/apsb
www.sciencedirect.com

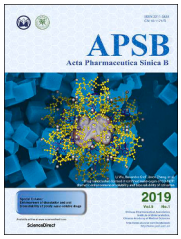

ORIGINAL ARTICLE

PARylation promotes acute kidney injury *via* RACK1 dimerization-mediated HIF-1α degradation

Xiangyu Li[a,†], Xiaoyu Shen[a,†], Xinfei Mao[b,c,†], Yuqing Wang[a,†], Yuhang Dong[a], Shuai Sun[d,e,f], Mengmeng Zhang[a], Jie Wei[g], Jianan Wang[a], Chao Li[a], Minglu Ji[a], Xiaowei Hu[h], Xinyu Chen[a], Juan Jin[i], Jiagen Wen[a], Yujie Liu[j], Mingfei Wu[b,c,*], Jutao Yu[a,*], Xiaoming Meng[a,*]

[a]*Inflammation and Immune Mediated Diseases Laboratory of Anhui Province, the Key Laboratory of Anti-Inflammatory of Immune Medicines, Ministry of Education, Anhui Institute of Innovative Drugs, School of Pharmaceutical Sciences, Anhui Medical University, Hefei 230032, China*
[b]*Key Laboratory of Neuropsychiatric Drug Research of Zhejiang Province, School of Pharmacy, Hangzhou Medical College, Hangzhou 310014, China*
[c]*Hangzhou Institute of Innovative Medicine, Institute of Drug Discovery and Design, College of Pharmaceutical Sciences, Zhejiang University, Hangzhou 310058, China*
[d]*Department of Urology, the First Affiliated Hospital of Anhui Medical University, Hefei 230032, China*
[e]*Institute of Urology, Anhui Medical University, Hefei 230032, China*
[f]*Anhui Province Key Laboratory of Urological and Andrological Diseases Research and Medical Transformation, Anhui Medical University, Hefei 230032, China*
[g]*Department of Nephrology, the Second Affiliated Hospital of Anhui Medical University, Hefei 230601, Anhui, China*
[h]*Department of Clinical Pharmacy, Anhui Provincial Children's Hospital, Hefei 230051, China*
[i]*Department of Pharmacology, School of Pharmaceutical Sciences, Key Laboratory of Anti-inflammatory and Immunopharmacology, Ministry of Education, Anhui Medical University, Hefei 230032, China*
[j]*Department of Obstetrics and Gynecology, the First Affiliated Hospital of USTC, University of Science and Technology of China, Hefei 230026, China*

Received 14 March 2025; received in revised form 9 April 2025; accepted 23 May 2025

*Corresponding authors.
E-mail addresses: mengxiaoming@ahmu.edu.cn (Xiaoming Meng), yujutao@ahmu.edu.cn (Jutao Yu), wmfayd@163.com (Mingfei Wu).
[†]These authors made equal contributions to this work.
Peer review under the responsibility of Chinese Pharmaceutical Association and Institute of Materia Medica, Chinese Academy of Medical Sciences.

https://doi.org/10.1016/j.apsb.2025.07.019

KEY WORDS

PARylation;
PARP1;
Acute kidney injury;
Inflammation;
RACK1;
Phosphorylation;
Dimerization;
HIF-1α

Abstract Poly(ADP-ribosyl)ation (PARylation) is a specific form of post-translational modification (PTM) predominantly triggered by the activation of poly-ADP-ribose polymerase 1 (PARP1). However, the role and mechanism of PARylation in the advancement of acute kidney injury (AKI) remain undetermined. Here, we demonstrated the significant upregulation of PARP1 and its associated PARylation in murine models of AKI, consistent with renal biopsy findings in patients with AKI. This elevation in PARP1 expression might be attributed to trimethylation of histone H3 lysine 4 (H3K4me3). Furthermore, a reduction in PARylation levels mitigated renal dysfunction in the AKI mouse models. Mechanistically, liquid chromatography-mass spectrometry indicated that PARylation mainly occurred in receptor for activated C kinase 1 (RACK1), thereby facilitating its subsequent phosphorylation. Moreover, the phosphorylation of RACK1 enhanced its dimerization and accelerated the ubiquitination-mediated hypoxia inducible factor-1α (HIF-1α) degradation, thereby exacerbating kidney injury. Additionally, we identified a PARP1 proteolysis-targeting chimera (PROTAC), **A19**, as a PARP1 degrader that demonstrated superior protective effects against renal injury compared with PJ34, a previously identified PARP1 inhibitor. Collectively, both genetic and drug-based inhibition of PARylation mitigated kidney injury, indicating that the PARylated RACK1/HIF-1α axis could be a promising therapeutic target for AKI treatment.

1. Introduction

Acute kidney injury (AKI) is characterised by a rapid increase in serum creatinine, a decline in urine output, or both[1,2]. It is a subset of conditions collectively referred to as acute kidney diseases and disorders (AKD), in which gradual deterioration of kidney function or persistent dysfunction is linked to irreversible loss of kidney cells and nephrons, potentially progressing to chronic kidney disease (CKD)[3]. AKI occurs in approximately 10%−15% of hospitalised patients, and its incidence is reported to exceed 50% in those in intensive care[4]. Tubular epithelial cells (TECs), the predominant cell type in the renal parenchyma, play a crucial role in regulating both physiological and pathological processes in the kidney[5,6]. Injury to TECs is a key determinant of the functional decline in AKI, serving as the initiating event[7]. Therefore, identifying the key regulatory factors in AKI pathology and developing targeted therapeutic strategies are critical objectives in the development of effective treatments for AKI.

Post-translational modifications (PTMs) may take place on particular amino acids within the regulatory domains of target proteins and play a key role in controlling protein stability[8]. Poly (ADP-ribosyl)ation (PARylation), a relatively new PTM, is primarily mediated by poly-ADP-ribose polymerase (PARP)[9]. PARP1 accounts for over 90% of cellular PARylation in non-neural tissues[10−13] and catalyses PARylation using nicotinamide adenine dinucleotide (NAD^+) as a co-substrate[14]. The extensive branching network of poly(ADP-ribose) (PAR) on PARP1 attracts and facilitates the assembly of multi-protein complexes involved in chromatin remodelling, DNA repair, damage checkpoint signalling, genomic stability, and programmed cell death[15,16]. Despite the growing understanding of its fundamental molecular functions, the physiological relevance and significance of PARylation in AKI remain poorly understood. Consequently, gaining a deeper understanding of the dynamics and spectrum of PARylation, as well as exploring its functional significance in diseases, could facilitate the development of effective strategies for intervention, prevention, and treatment.

In this study, we found that PARylation was consistently elevated in both human biopsies and murine models of AKI, and it correlated with kidney inflammation and injury. Therefore, we postulated that PARylation might regulate AKI. Our hypothesis was evaluated *in vivo* in mice with adeno-associated virus (AAV)-mediated *Parp1* knockdown and *in vitro* in *PARP1*-overexpressed and *PARP1*-silenced TECs. Additionally, PDD was used to increase the level of PARylation both *in vivo* and *in vitro*. Then, we performed liquid chromatography-mass spectrometry (LC−MS/MS) analyses and co-immunoprecipitation (Co-IP) to investigate the mechanism of PARylation in AKI. Furthermore, we evaluated the efficacy of PARylation-targeted therapy in the mouse model of AKI. These findings reveal a potential therapy for AKI and identify a promising drug candidate for treating PARylation-mediated diseases.

2. Materials and methods

2.1. Study design

This study aimed to examine the role of PARylation in AKI pathogenesis and to uncover the molecular mechanisms involved. Our study utilized a multifaceted strategy that included human kidney tissue samples, different murine models of AKI, and *in vitro* models of renal tubular cell damage to explore the role of PARylation. Patients diagnosed with AKI and acute tubular necrosis, confirmed through renal biopsy, at the First Affiliated Hospital of Anhui Medical University were included in this study. For analyzing PARylation expression in kidney tissues, non-tumor kidney tissue from patients who underwent nephrectomy for renal cell carcinoma served as the normal control. In animal studies, we used littermates whenever possible, which facilitated randomisation. Based on our experience with similar studies, the sample size for animal research was determined using statistical analysis of variance (ANOVA). The sample size (n) for each experimental group was between six and eight mice per group. Within the littermate groups, AKI was induced by exposure to cisplatin (CIS) and ischaemia/reperfusion (I/R) in mice with or without

Please cite this article as: Li Xiangyu et al., PARylation promotes acute kidney injury *via* RACK1 dimerization-mediated HIF-1α degradation, Acta Pharmaceutica Sinica B, https://doi.org/10.1016/j.apsb.2025.07.019

Parp1 knockdown. A PAR glycohydrolase (PARG) inhibitor named PDD and the PARP1 PROTAC **A19** were used. In cell studies, a minimum of three experimental replicates were performed in TECs with knockdown or overexpression of *PARP1* and knockdown of receptor for activated C kinase 1 (*RACK1*). Figure legends include the number of replicates. All immunohistochemical (IHC) analyses were carried out by two independent pathologists in a blinded manner. Statistical tests were selected based on the nature of variables, assumption of data distribution, and effect size.

2.2. Reagents and materials

The sources and catalogue numbers of the antibodies used were as follows: KIM-1 (bs-21420R) was purchased from Bioss (Beijing, China), p-P65 (#3033) and P65 (#8242) were obtained from Cell Signaling Technology (Beverly, USA), PARP1 (66520-1-Ig) and FLAG (20543-1-AP) were obtained from Proteintech (Rosemont, IL, USA), MYC (R1208-1) and Histone H3 (M1309-1) were purchased from Huabio (Hangzhou, China), RACK1 (sc-17754) was purchased from Santa Cruz Biotechnology (Dallas, TX, USA), PAR/pADPr (4335-MC-100) was purchased from R&D Systems (Minnesota, USA), HIF-1α (YT2133) and Phosphoserine (YP1878) were obtained from Immunoway (Plano, USA), H3K4me3 (A22146) was purchased from ABclonal (Wuhan, China), ubiquitin (382766) was purchased from ZENBIO (Chengdu, China), Fluorescein-labelled LTL (FL-1321) was purchased from Vector Laboratories (Newark, CA, USA), PARP2 (CY8141) and HIF-2α (CY5098) were obtained from Abways (Shanghai, China), PARP5a (BD-PN2269) and PARP5b (BD-PN2396) were obtained from Biodragon (Suzhou, China), and β-actin (GB12001-100) was purchased from Servicebio (Wuhan, China). MM102 (B1582), OICR9429 (B6168), and PJ34 (A3729) were purchased from APExBIO. PDD (HY-108360) and DMOG (HY-15893) were purchased from MedChemExpress (Monmouth Junction, NJ, USA). Cisplatin (p4393) was purchased from Sigma−Aldrich (St. Louis, MO, USA). Hematoxylin and eosin (HE), Periodic acid−Schiff (PAS), creatinine (CRE), and blood urea nitrogen (BUN) assay kits were obtained from Jiancheng Bioengineering Institute (Nanjing, China). NAD^+/NADH assay kit was purchased from Beyotime (Shanghai, China).

2.3. Animal studies

All animal experiments were performed by the Guide for the Care and Use of Laboratory Animals. Six-to eight-week-old male C57BL/6J mice (approximately 20−22 g) were provided by the Experimental Animal Center, Anhui Medical University. All animal experiments were conducted at Anhui Medical University, and all animal procedures were approved by the Animal Experimentation Ethics Committee of Anhui Medical University, Anhui, China (LLSC20242231). For CIS-induced AKI, the mice were intraperitoneally injected with a single dose of CIS (20 mg/kg). All animals were sacrificed under anaesthesia three days after injection. For the PDD treatment, 10 mg/kg PDD was administered *via* intraperitoneal injection 12 h before CIS administration. For the **A19** treatment, **A19** (2.5, 5, or 10 mg/kg) was administered *via* intraperitoneal injection 12 h before CIS administration and then injected once daily thereafter. For I/R-induced AKI, renal I/R was induced in mice as previously described[17]. In brief, mice were anaesthetised and placed on a thermostat plate to maintain the body temperature at 36.5 °C. Bilateral renal pedicles were clipped for 40 min using microaneurysm clamps. After ischaemia, the clamps were released for 24 h of reperfusion, and all animals were sacrificed under anaesthesia. Sham control animals were subjected to an identical procedure without renal pedicle clamping. For AAV9-mediated *Parp1* knockdown in mice, the AAV were developed and supplied by Hanheng (Shanghai, China). The serotype of AAV was AAV2/9, and the vector was constructed using the Ksp-cadherin promoter, incorporating the woodchuck hepatitis virus posttranscriptional regulatory element (WPRE) to enhance gene expression. The mice were injected slowly with 100 μL of AAV9-packaged *Parp1* knockdown plasmid (1×10^{12} vg/mL) through the tail vein, as previously reported[18]. The kidney tissue and blood samples were collected for further analyses. Blood samples were collected for BUN and CRE measurements, according to the manufacturer's instructions. The kidneys were collected for paraffin embedding, molecular analysis, and electron microscopy. Paraffin sections, 4 μm thick, were stained with a PAS staining kit (Fuzhou Maixin Biotech Co., Ltd.). At least six to eight mice were used in each group.

2.4. Cell lines and culture conditions

The human kidney tubular epithelial cell line, HK2, was obtained from Prof. Hui Yao Lan at The Chinese University of Hong Kong, as previously noted[19,20]. TECs were cultured in 5% FBS-containing HyClone™ DMEM/F12 medium in a 95% air and 5% CO_2 atmosphere. After overnight starvation in DMEM/F12 medium with 0.5% FBS, HK2 cells were treated with CIS (20 μmol/L) for 24 h. For hypoxia reoxygenation (H/R) injury, TECs were incubated in glucose-free medium in a tri-gas incubator (94% N_2, 5% CO_2, and 1.0% O_2) at 37 °C for 12 h. Subsequently, the cells were returned to complete medium under normal conditions for 6 h for reoxygenation.

2.5. Human specimens

Human kidney biopsy sections, embedded in paraffin and measuring 3−4 μm in thickness, were prepared following standard procedures. This study was approved by the Biomedical Ethics Committee of Anhui Medical University (81250522). The experiments were conducted with the informed written consent of each participant. All protocols adhered to the principles outlined in the Declaration of Helsinki.

2.6. Immunofluorescence staining

Embedded kidney tissue sections (4 μm thick) were dewaxed and returned to room temperature after antigen retrieval using 1 × EDTA working solution diluted from 50 × EDTA repair solution (pH = 8.0) (G1206-250 mL, Servicebio). Alternatively, the cells were attached to coverslips and fixed with paraformaldehyde. The samples were incubated overnight with the desired primary antibodies in 10% bovine serum albumin solution. After washing with phosphate-buffered saline, the samples were incubated for 2 h at room temperature with goat anti-rabbit IgG-rhodamine and goat anti-mouse IgG-rhodamine secondary antibodies (Bioss). The tissue sections and cells were counterstained with DAPI and visualised under a fluorescence microscope (Leica, Bensheim, Germany).

Please cite this article as: Li Xiangyu et al., PARylation promotes acute kidney injury *via* RACK1 dimerization-mediated HIF-1α degradation, Acta Pharmaceutica Sinica B, https://doi.org/10.1016/j.apsb.2025.07.019

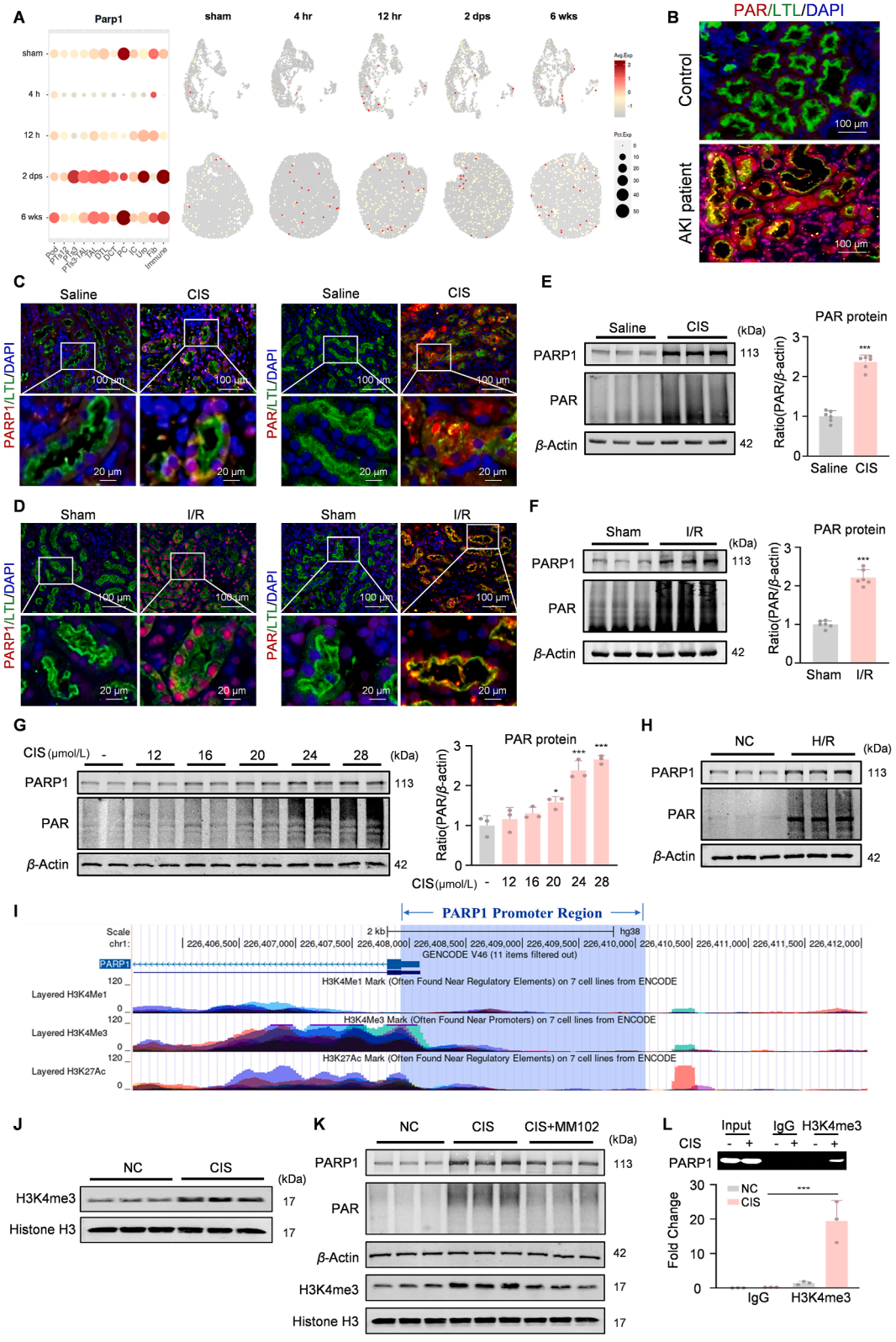

Figure 1 The levels of PARP1 and PARylation increase in biopsy samples, mouse models, and TECs in response to different AKI stimuli *via* H3K4me3 modification. (A) Single-cell sequencing results of mouse ischemia-reperfusion injury models of renal injury at different stages. Pod: podocytes; PTs1, PTs2, PTs3: proximal tubule segment 1, 2, 3; TAL: thick ascending limb; DTL: descending thin limb; DCT: distal convoluted tubule; PC: principal cells; IC: intercalated cells; Uro: urothelial cells; Fib: fibroblasts; Immune: immune cells; (B) Representative IF staining data on PAR in kidney biopsies from patients with AKI; (C, D) IF staining of PARP1 and PAR with LTL in CIS- and I/R-induced AKI mouse model; (E, F) Western blot analysis of PARP1 and PAR proteins in CIS- and I/R-induced AKI mouse model ($n = 6$, *t*-test); (G, H) Western blot analysis

Please cite this article as: Li Xiangyu et al., PARylation promotes acute kidney injury *via* RACK1 dimerization-mediated HIF-1α degradation, Acta Pharmaceutica Sinica B, https://doi.org/10.1016/j.apsb.2025.07.019

2.7. Renal histology and immunohistochemistry

Paraffin-embedded mouse kidney sections were prepared using routine procedures, including fixation, dehydration, waxing, and embedding (4 μm). PAS and H&E staining were performed, and histological examinations were performed using light microscopy. Renal tubular injury was scored as previously described[17,21]. IHC staining was performed according to the manufacturer's instructions. The desired primary antibody was incubated overnight at 4 °C, and the secondary antibodies were incubated for 1 h at room temperature. After staining with diaminobenzidine and counterstaining with haematoxylin, the sections were visualised under a microscope (Olympus IX83, Japan).

2.8. Overexpression and knockdown of genes

Transfection of plasmids or siRNA was performed using jetPRIME (Polyplus) according to the manufacturer's instructions, followed by analysis 48−72 h later. The selected sequences are listed in Supporting Information Table S1.

2.9. Western blot analysis

Protein lysates from kidney tissues and cultured cells were prepared following standard protocols, and Western blot analysis was performed as described previously[19,22,20]. Samples were incubated with primary antibodies for 12 h at 4 °C and subsequently incubated with IRDye 800-conjugated secondary antibody (1:10,000) for 1.5 h at room temperature. Images were captured using a Li-Cor/Odyssey infrared imaging system (LI-COR Biosciences, Lincoln, NE, USA) and were normalized and analysed in gray-scale images. Then, images were quantified using ImageJ software (NIH, Bethesda, MD, USA).

2.10. RNA isolation and quantitative real-time PCR

Total RNA was extracted from cells or tissues using the TRIzol reagent (15596018, Invitrogen, Waltham, MA, USA), following the manufacturer's instructions. Real-time PCR was performed using Bio-Rad iQ SYBR Green Supermix on an Opticon 2 real-time PCR detection system (Bio-Rad) using a CFX96 real-time PCR detection system, as previously described[23]. The primer sequences are listed in Supporting Information Table S2.

2.11. Cell viability assay

Cell viability was determined using the MTT assay, based on the principle of purple formazan product formation by mitochondrial dehydrogenase, which is present in viable cells. Briefly, HK2 cells were seeded in 96-well plates and cultured with different known concentrations of PDD and **A19** for 24 h. Subsequently, 5 mg/mL MTT solution was added to each well, and the cells were incubated at 37 °C for 4 h. After incubation, the supernatant was removed, and 150 μL of dimethyl sulfoxide (DMSO) was used to dissolve the formazan crystals. Optical density (OD) was measured at a wavelength of 492 nm (Multiskan MK3; Thermo Fisher Scientific Corp.).

2.12. Chromatin immunoprecipitation assay

Chromatin immunoprecipitation (ChIP) was performed using the SimpleChIP Enzymatic Chromatin IP Kit (#9003, Cell Signaling Technology) according to the manufacturer's instructions. The following antibodies were used for immunoprecipitation: a mouse polyclonal antibody specific for PARP1, a rabbit polyclonal antibody specific for H3K4me3, and normal rabbit IgG as a negative control for non-specific binding. Subsequently, a set of specific primers was used to purify the immunoprecipitated DNA, which was then analysed using PCR to quantify the enriched target DNA sequences.

2.13. Co-immunoprecipitation

Co-IP analysis was performed as described previously[21]. Briefly, the cells were washed three times with ice-cold phosphate-buffered saline and lysed in 1% NP-40 buffer. The samples were precipitated with PARP1, RACK1, and HIF-1α antibodies (1 μg) and protein A/G−agarose beads (Santa Cruz Biotechnology) by incubation at 4 °C overnight. The bound proteins were removed by boiling in SDS buffer and resolved on 4%−20% SDS-polyacrylamide gels for Western blot analysis with PARP1, RACK1, PAR/pADPr, phosphoserine, MYC, and FLAG antibodies.

2.14. Identification of PAR-interacting proteins by LC−MS/MS analysis

HK2 cells were treated with CIS and a *PARP1* overexpression plasmid. Cell lysates were immunoprecipitated using anti-PAR/pADPr and protein A/G magnetic beads. Proteins were resolved by SDS-PAGE, reduced, alkylated, and digested with trypsin in situ. Tryptic peptides were analyzed using a Q Exactive HF mass spectrometer (Thermo Fisher Scientific, Waltham, MA, USA). LC−MS/MS detection and analysis were conducted by Shanghai Luming Biological Technology Co., Ltd. (Shanghai, China).

2.15. Transmission electron microscopy

The cell samples were immersed in 2.5% glutaraldehyde in 0.1 mol/L sodium cacodylate (pH 7.4) at 4 °C overnight, and postfixed for 2 h in buffered 1% osmium tetroxide on ice. After staining and fixation with 2% uranium acetate (pH 7.4) for 2 h, the specimens were dehydrated in a graded series of ethanol (50%, 70%, 90%, and 100%) and 100% acetone and subsequently embedded in EPON 812 resin. Polymerisation was achieved in gelatin capsules at 60 °C for 48 h and then sliced at a thickness of 70−100 nm. The samples were then analysed using transmission electron microscopy (Thermo Scientific Talos L120C G2).

of PARP1 and PAR proteins in HK2 cells treated with CIS and H/R ($n = 3$, one-way ANOVA); (I) Validation of PARP1 histone modification levels using the UCSC Genome Browser database; (J) Western blot analysis of H3K4me3 in CIS-treated HK2 cells ($n = 3$); (K) Western blot analysis of PARP1, PAR and H3K4me3 proteins after treatment with MM102 following CIS induction ($n = 3$); (L) ChIP assay for the binding of H3K4me3 to PARP1. Data are mean ± SD; $^*P < 0.05$, $^{**}P < 0.01$, $^{***}P < 0.001$ *vs*. Control/Model. Scale bar = 50 μm.

Please cite this article as: Li Xiangyu et al., PARylation promotes acute kidney injury *via* RACK1 dimerization-mediated HIF-1α degradation, Acta Pharmaceutica Sinica B, https://doi.org/10.1016/j.apsb.2025.07.019

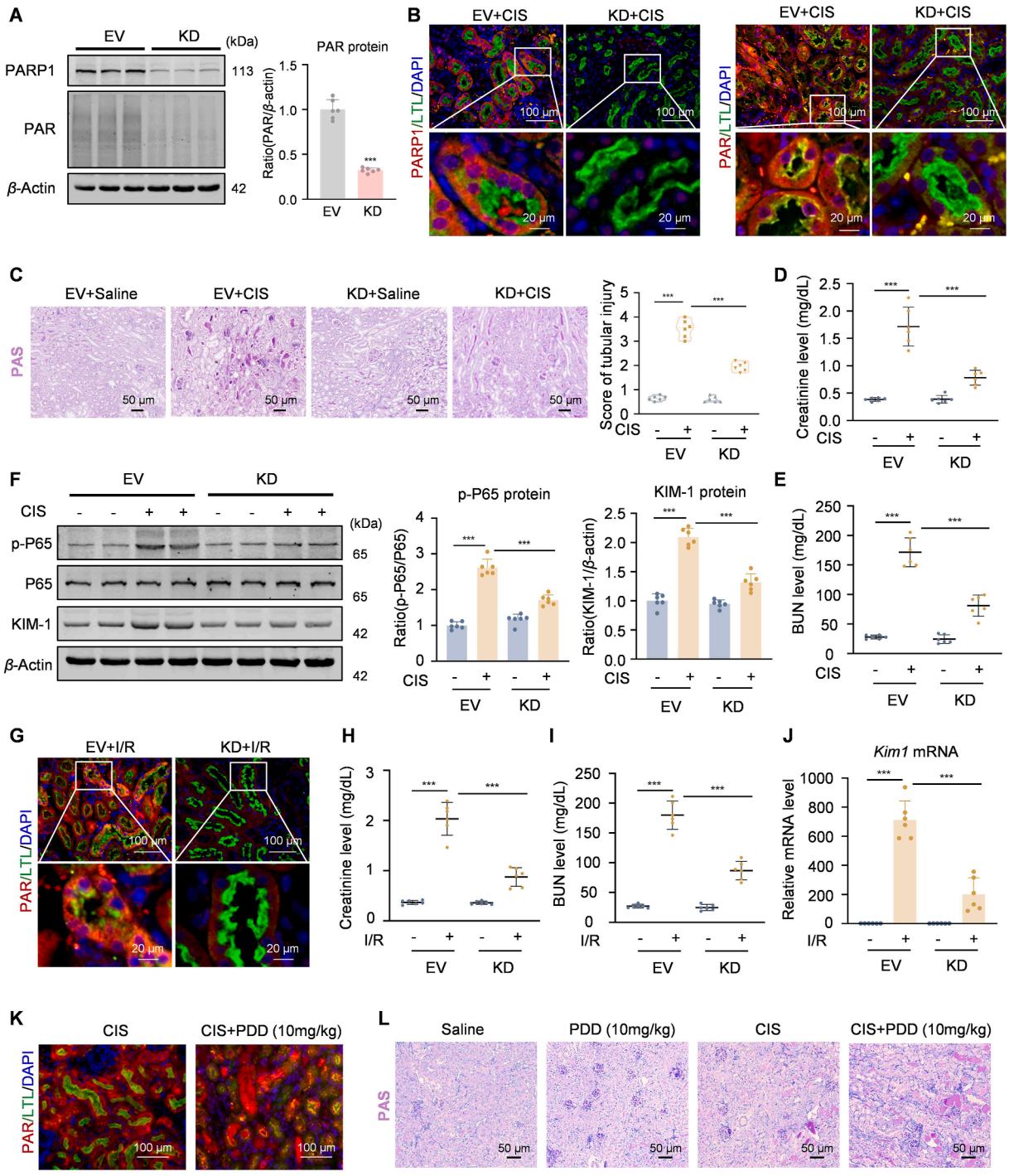

Figure 2 Decreased PARylation levels protect against kidney injury and inflammation in CIS- and I/R-induced mice with AKI, whereas an increase in PARylation levels exacerbates the damage. (A) Western blot analysis of PARP1 and PAR expression in mice with AAV-empty vector (EV) or AAV-PARP1 knockdown (KD) ($n = 6$, *t*-test); (B) Double staining of PARP1/PAR and LTL in mice with AAV-EV and AAV-PARP1 KD with CIS-induced AKI. Scale bar = 100 μm; (C) PAS staining indicating tubular injury in CIS-induced AKI mice with or without PARP1 KD. Scale bar = 50 μm; (D, E) Serum CRE and BUN in the CIS-induced AKI mouse model with or without PARP1 KD ($n = 6$, one-way ANOVA); (F) Western blot analysis of KIM-1, p-P65, and P65 in the CIS-induced AKI mouse model ($n = 6$, one-way ANOVA); (G) Double staining of PAR and LTL in the I/R-induced AKI mouse model with or without PARP1 KD. Scale bar = 100 μm; (H, I) Serum CRE and BUN in the I/R-induced AKI mouse model with or without PARP1 KD ($n = 6$, one-way ANOVA); (J) Real-time PCR analysis of *Kim1* mRNA levels in the I/R-induced AKI mouse model ($n = 6$, one-way ANOVA); (K) Double staining of PAR and LTL in PDD-treated mice with CIS-induced AKI. Scale bar = 100 μm; (L) PAS staining indicating tubular injury in mice with CIS-induced AKI with or without PDD. Scale bar = 50 μm. Data are mean ± SD; $^{*}P < 0.05$, $^{**}P < 0.01$, $^{***}P < 0.001$ *vs*. Control/Model.

Please cite this article as: Li Xiangyu et al., PARylation promotes acute kidney injury *via* RACK1 dimerization-mediated HIF-1α degradation, Acta Pharmaceutica Sinica B, https://doi.org/10.1016/j.apsb.2025.07.019

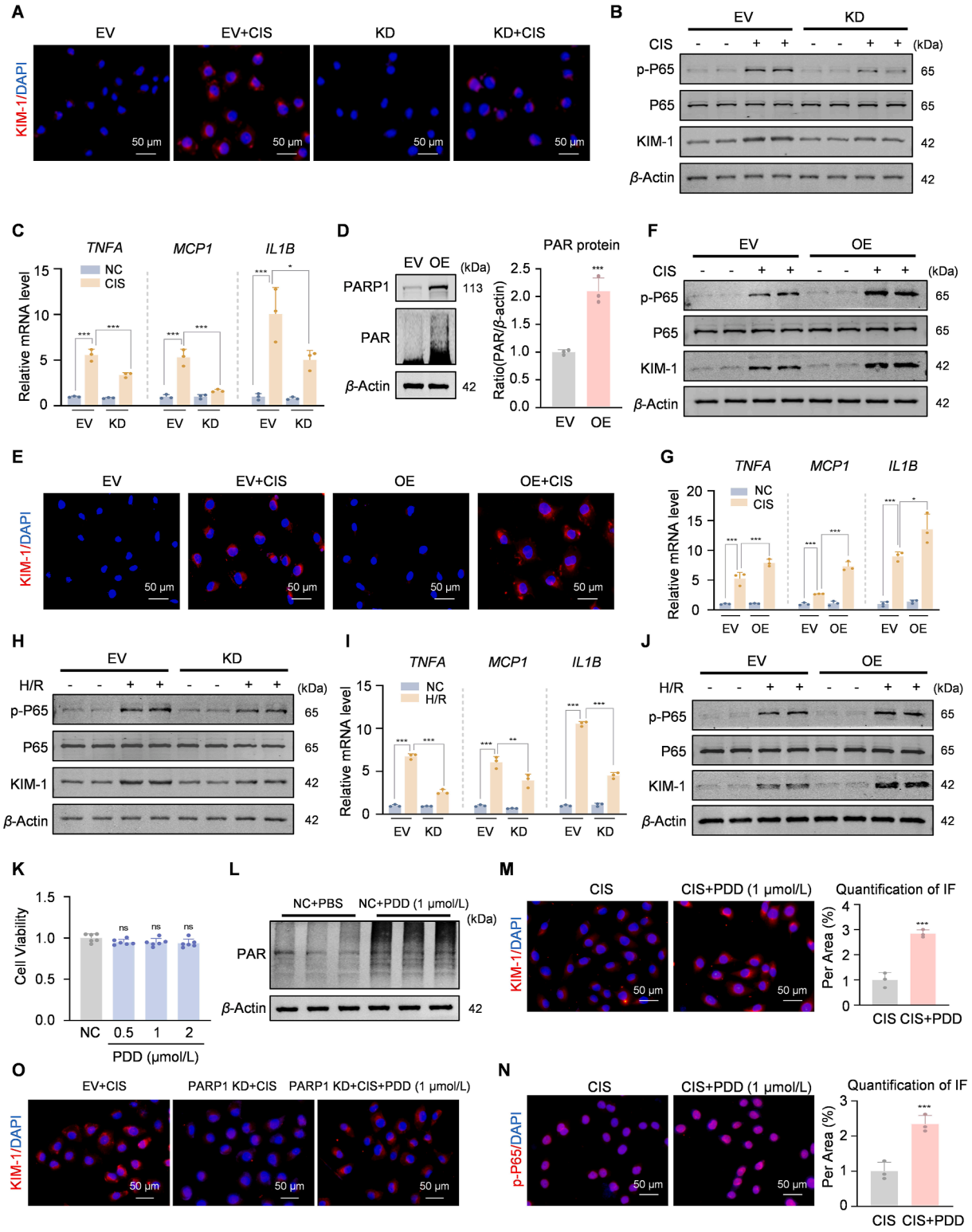

Figure 3 Reduction in PARylation levels *in vitro* alleviates CIS- and H/R-induced cell injury and inflammation, while the increase in PARylation levels reverses these effects. (A) IF staining of KIM-1 in CIS-induced cells with or without PARP1 KD. Scale bar = 50 μm; (B) Western blot analysis of KIM-1, p-P65, and P65 in CIS-induced cells with or without PARP1 KD (n = 3); (C) Real-time PCR analysis of *TNFA*, *MCP1*, and *IL1B* mRNA levels in CIS-induced cells with or without PARP1 KD (n = 3, one-way ANOVA); (D) PARP1 and PAR levels were confirmed by Western blot in HK2 cells (n = 3, t-test); (E) IF staining of KIM-1 in CIS-induced cells with or without PARP1 overexpression (OE). Scale bar = 50 μm; (F) Western blot analysis of KIM-1, p-P65, and P65 in CIS-induced cells with or without PARP1 OE (n = 3); (G) Real-time PCR analysis of *TNFA*, *MCP1*, and *IL1B* mRNA levels in CIS-induced cells with or without PARP1 OE (n = 3, one-way ANOVA); (H) Western blot analysis of KIM-1, p-P65, and P65 in H/R-induced cells with or without PARP1 KD (n = 3); (I) Real-time PCR analysis of *TNFA*, *MCP1*, and

Please cite this article as: Li Xiangyu et al., PARylation promotes acute kidney injury *via* RACK1 dimerization-mediated HIF-1α degradation, Acta Pharmaceutica Sinica B, https://doi.org/10.1016/j.apsb.2025.07.019

2.16. Synthesis of the PARP1-targeted PROTAC A19

The thalidomide derivative 3 was synthesized by heating a mixture of the commercially available fluorine-substituted phthalic anhydride derivative **1** and raw material **2**. Following this step, nucleophilic substitution involving the *N*-heterocyclic alkane derivative **4** in the presence of DIPEA yielded compound **5**. Then intermediate **5** was subsequently transformed into its corresponding aldehyde derivative **6** through the oxidation process using Dess-Martin periodinane (DMP) conditions. The Boc-piperidine fragment **8** and commercially available Niraparib **7** were subjected to a reduction-amination reaction to yield compound **9**. Intermediate **9** was deprotected to yield an imine fragment, which was reductively aminated with a Boc-piperidine fragment, resulting in intermediate **10**. Following additional deprotection, the imine fragment of **10** underwent reductive amination with intermediate **6**, yielding product **A19** (Supporting Information Methods, Supporting Information Scheme S1). The chemical structure of **A19** was verified by proton and carbon nuclear magnetic resonance (NMR) spectra, high-resolution mass spectrometry (HRMS) data, and HPLC chromatograms (Supporting Information Fig. S1).

2.17. NAD^+ assay

NAD^+ assay was performed using the NAD^+/NADH assay kit according to the manufacturer's instructions. In brief, for adherent cell samples, NAD^+/NADH extract was added, followed by centrifugation. The supernatant was collected as the test sample. Then, the standard solution and working solution were prepared. The samples were added to the 96-well plate according to experimental requirements. After incubation, the colorimetric solution was added. Finally, the absorbance at 450 nm was measured.

2.18. Statistical analysis

All statistical analyses were performed using SPSS version 23.0 (IBM Corp., Armonk, NY, USA). GraphPad Prism 8.0 (GraphPad Software Inc., La Jolla, CA, USA) was used to generate all figures. All results were tested for normal distribution using the Shapiro−Wilk method, and normal distribution quantitative data are reported as the mean ± standard deviation (SD). Independent sample *t*-test and one-way ANOVA followed by Tukey's *post hoc* test were used to examine the differences in the means of different groups. Statistical significance was set at $P < 0.05$.

3. Result

3.1. PARylation is significantly increased in human biopsies, mouse models, and TECs in response to AKI

First, we reanalysed the single-cell sequencing results of mouse I/R injury models of renal injury at different stages[24]. The results confirmed that the expression of PARP1, the main enzyme that catalyses PARylation, was significantly increased during both renal injury and repair (http://humphreyslab.com/SingleCell/) (Fig. 1A). Immunofluorescence (IF) demonstrated a marked increase in PARylation levels from patients with AKI (Fig. 1B). Importantly, PARylation and PARP1 were mainly localised in the renal tubules of mice with CIS- and I/R-induced AKI (Fig. 1C and D). PARylation and PARP1 expression were consistently upregulated at the protein level in response to CIS and I/R (Fig. 1E and F, Supporting Information Fig. S2A and S2B). *In vitro* experiments validated the findings observed *in vivo*, showing that PARylation and PARP1 were induced at both the mRNA and protein levels in CIS- and H/R-treated HK2 cells (Fig. 1G and H, Fig. S2C−S2F).

In addition to PARP1, other PARP family enzymes, including PARP2, PARP5a, and PARP5b, may also induce PARylation. We examined changes in their expression in the AKI model. In the CIS-induced HK2 cells, the level of *PARP5a* did not change significantly, but the level of *PARP2* and *PARP5b* increased (Fig. S2G−S2I). Therefore, we knocked down *PARP1*, *PARP2*, and *PARP5b*, respectively, to explore their effects on PAR expression levels. Western blot and real-time PCR analyses confirmed that *PARP1* was successfully knocked down in HK2 cells, and the PARylation level was significantly reduced (Fig. S2J and S2K). In contrast, there was no significant change in PARylation levels after *PARP2* and *PARP5b* were knocked down, respectively (Fig. S2L−S2O). Therefore, we further identify PARP1 as the main enzyme mediating PARylation in AKI.

To investigate the mechanisms driving the upregulation of PARP1 in AKI, we performed a comprehensive analysis using the UCSC Genome Browser database (https://genome.ucsc.edu/). Our analysis suggested that the promoter region of *PARP1* was subjected to epigenetic modifications, and the peak for trimethylation of histone H3 lysine 4 (H3K4me3) was the highest (Fig. 1I). Consistent with this hypothesis, we observed a significant increase in the H3K4me3 levels in CIS-treated HK2 cells *in vitro* (Fig. 1J, Supporting Information Fig. S3A). The H3K4me3 methyltransferase mixed-lineage leukemia 1 (MLL1) is activated on forming a complex with WD-40 repeat protein 5, and both MM102 and OICR9429 are known to inhibit the activity of the MLL1/WD-40 repeat protein 5 complex[25]. Following treatment with MM102 and OICR9429, we observed a lack of methylation at H3K4, which significantly diminished the upregulation of *PARP1* mRNA and total protein levels, along with reduced PARylation levels (Fig. 1K; Fig. S3B−S3E). In addition, we used *MLL1* siRNA to effectively reduce H3K4me3 levels, and the results showed that the expression levels of PARP1 and PAR were also reduced (Fig. S3F and S3G). Furthermore, ChIP assay provided compelling evidence that H3K4me3 modification directly targeted PARP1, which might result in increased PARylation (Fig. 1L).

3.2. PARylation deletion protects against CIS- and I/R-induced kidney injury and inflammation

To investigate the function of PARylation in AKI mouse models, we silenced *Parp1* in mice using an AAV9-packaged *Parp1*

IL1B mRNA levels in H/R-induced cells with or without PARP1 KD ($n = 3$, one-way ANOVA); (J) Western blot analysis of KIM-1, p-P65, and P65 in H/R-induced cells with or without PARP1 OE ($n = 3$); (K) MTT cell survival assay of HK2 cells at different PDD doses; (L) Western blot analysis of PAR expression in PDD-treated HK2 cells ($n = 3$); (M) IF staining of KIM-1 in CIS-induced cells with or without PDD. Scale bar = 50 μm; (N) IF staining of p-P65 in CIS-induced cells with or without PDD. Scale bar = 50 μm; (O) IF staining of KIM-1 after PDD treatment in CIS-induced PARP1 KD cells. Scale bar = 50 μm. Data are mean ± SD; $^*P < 0.05$, $^{**}P < 0.01$, $^{***}P < 0.001$ *vs*. Control/Model; ns stands for not significant with *P* value greater than 0.05.

Please cite this article as: Li Xiangyu et al., PARylation promotes acute kidney injury *via* RACK1 dimerization-mediated HIF-1α degradation, Acta Pharmaceutica Sinica B, https://doi.org/10.1016/j.apsb.2025.07.019

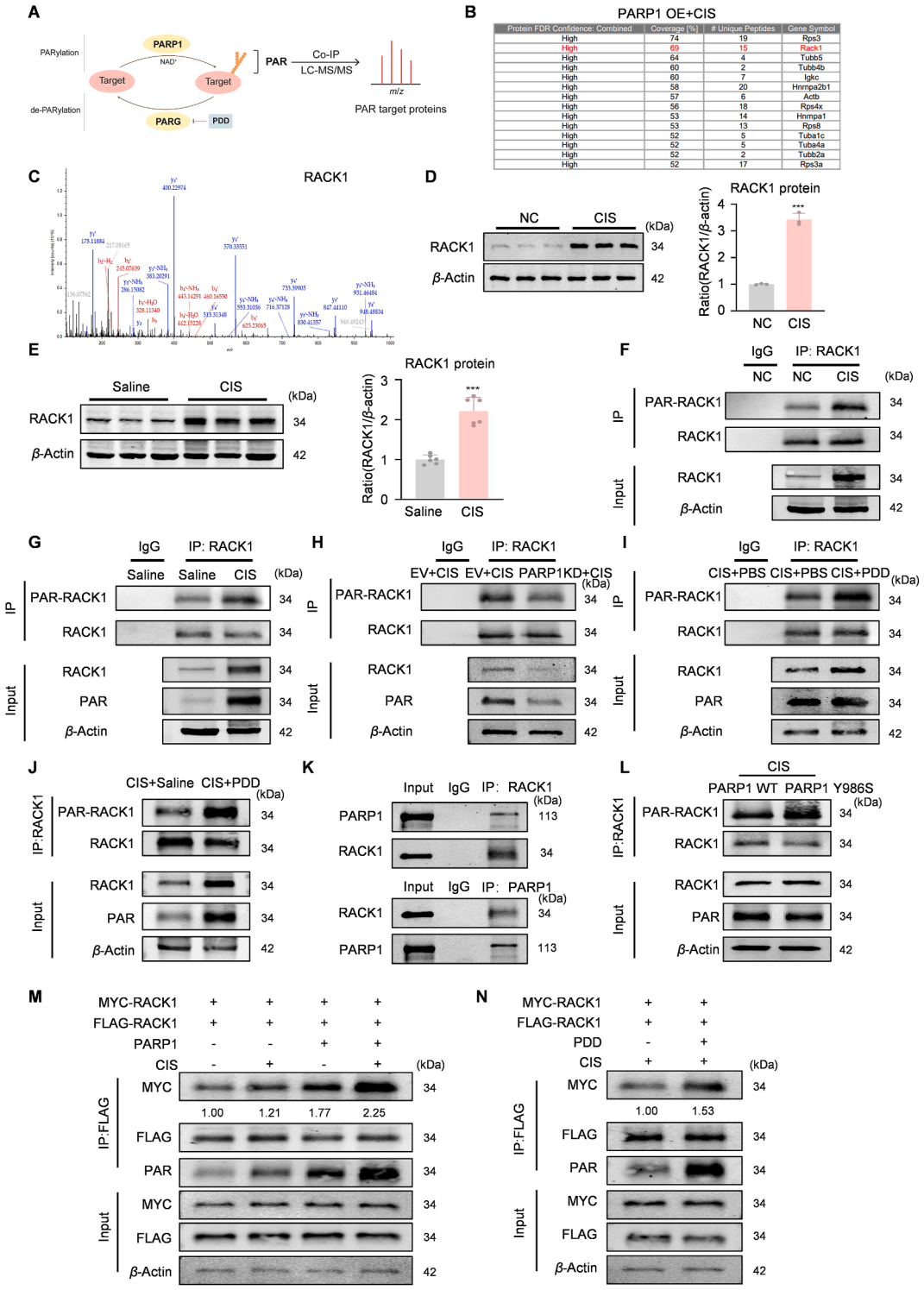

Figure 4 PAR chains primarily bind to RACK1 and promote its dimerization. (A) Flow chart showing identification of PARylated acceptor proteins; (B, C) LC−MS/MS analysis of RACK1 showing relatively high binding score of PAR and RACK1; (D) Western blot analysis of RACK1 in CIS-induced HK2 cells ($n = 3$, *t*-test); (E) Western blot analysis of RACK1 in CIS-induced AKI mice ($n = 6$, *t*-test); (F) Co-IP assay indicates the level of PARylated RACK1 in CIS-induced HK2 cells; (G) Co-IP assay indicates the level of PARylated RACK1 in CIS-induced AKI mice; (H) Co-IP assay indicates the level of PARylated RACK1 in CIS-induced PARP1 KD cells; (I) Co-IP assay indicates the level of PARylated RACK1 in CIS-induced cells treated with PDD; (J) Co-IP assay indicates the level of PARylated RACK1 in CIS-induced AKI mice treated with PDD; (K) Co-IP assay indicates the interactions of PARP1 and RACK1; (L) Co-IP assay indicates the level of PARylated RACK1 in CIS-induced PARP1 Y986S cells; (M, N) Co-IP assay indicates the influence of PARP1 and PDD on the dimerization of RACK1 in CIS-induced HK2 cells. Data are mean ± SD; $^{*}P < 0.05$, $^{**}P < 0.01$, $^{***}P < 0.001$ *vs*. Control.

Please cite this article as: Li Xiangyu et al., PARylation promotes acute kidney injury *via* RACK1 dimerization-mediated HIF-1α degradation, Acta Pharmaceutica Sinica B, https://doi.org/10.1016/j.apsb.2025.07.019

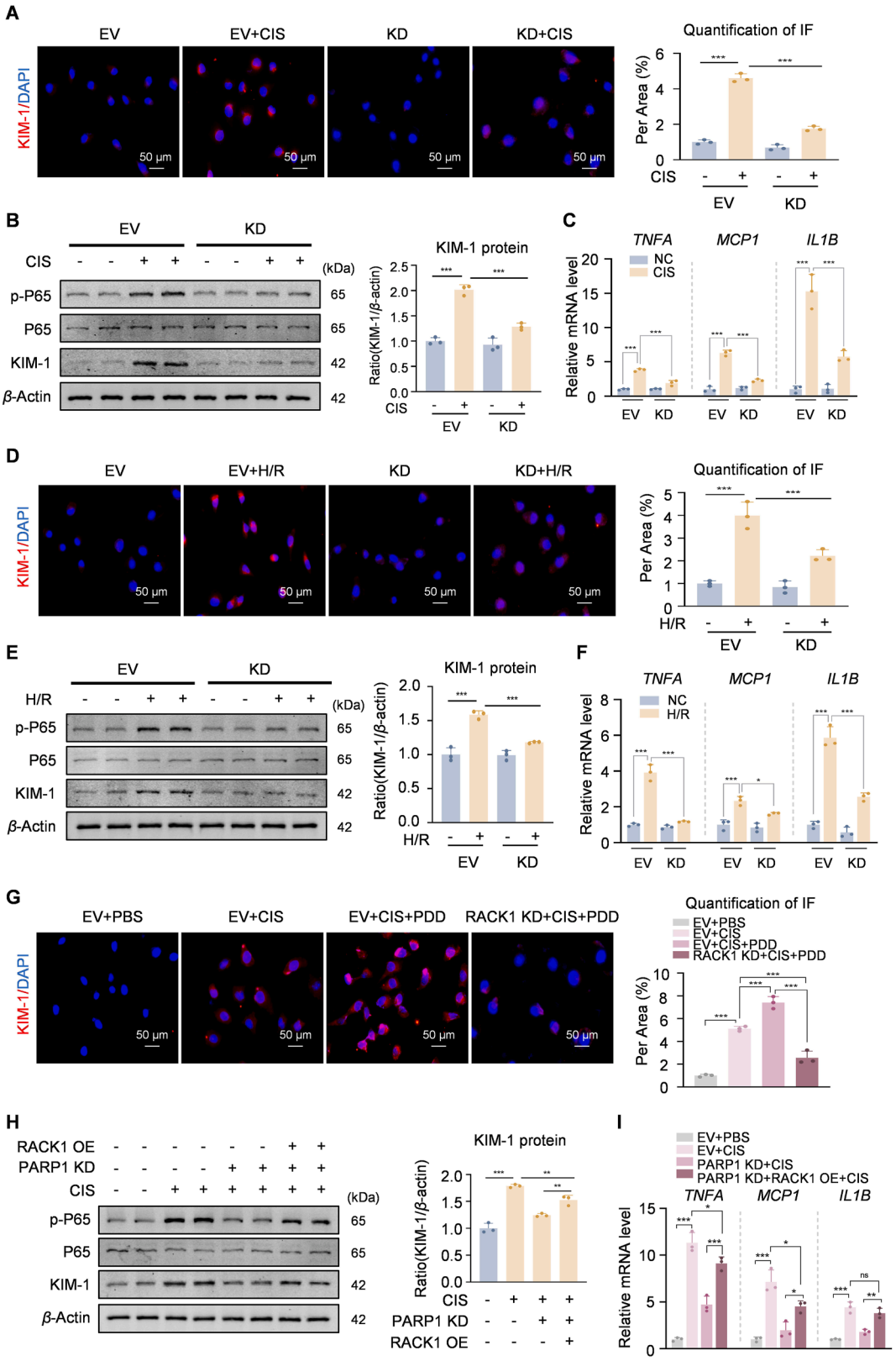

Figure 5 Silencing of RACK1 can alleviate the damage and inflammation in HK2 cells treated with CIS and H/R, and PARylation exerts its effects by targeting RACK1. (A) IF staining of KIM-1 in CIS-induced cells with or without RACK1 KD. Scale bar = 50 μm; (B) Western blot analysis of KIM-1, p-P65, and P65 in CIS-induced cells with or without RACK1 KD (n = 3, one-way ANOVA); (C) Real-time PCR analysis of *TNFA*, *MCP1*, and *IL1B* mRNA levels in CIS-induced cells with or without RACK1 KD (n = 3, one-way ANOVA); (D) IF staining of KIM-1 in H/R-induced cells with or without RACK1 KD. Scale bar = 50 μm; (E) Western blot analysis of KIM-1, p-P65, and P65 in H/R-induced cells

knockdown plasmid (Supporting Information Fig. S4A). Western blot and IF analyses showed that *Parp1* was successfully knocked down in CIS-induced kidney damage and that the level of PARylation decreased (Fig. 2A and B, Fig. S4B and S4C). PAS staining revealed that a decrease in PARylation prevented kidney damage in the mice (Fig. 2C). These results were confirmed by CRE and BUN, which indicate the degree of renal injury (Fig. 2D and E). Western blot and real-time PCR showed that loss of PARylation resulted in reduced kidney injury molecule 1 (KIM-1) expression and p65 nuclear factor κB (P65NF-κB) phosphorylation, as well as lower production of inflammatory cytokines (tumor necrosis factor α (*Tnfa*), monocyte chemoattractant protein-1 (*Mcp1*), and interleukin-1β (*Il1b*)) in mice with CIS-induced AKI (Fig. 2F, Fig. S4D and S4E).

Next, we examined the function of PARylation in I/R-induced AKI. IF analysis showed that *Parp1* was successfully knocked down in I/R-induced kidney damage and that the level of PARylation decreased (Fig. 2G, Fig. S4F). Our results demonstrated that the lack of PARylation significantly alleviated I/R-induced kidney dysfunction and tubular damage, as evidenced by serum CRE and BUN, PAS, Western blot, and real-time PCR (Fig. 2H–J, Fig. S4G–S4J).

Furthermore, we used a potent PARG inhibitor, PDD, to augment PARylation by inhibiting PAR degradation. The mice were pre-treated with PDD (10 mg/kg) 12 h before CIS injection. IF analysis showed that the level of PARylation was increased (Fig. 2K). Elevated PARylation exacerbated the CIS-induced upregulation of serum CRE and BUN concentrations, and PAS staining highlighted the extent of renal damage (Fig. 2L, Fig. S4K–S4M). Collectively, our data suggest that PARylation is a critical PTM that contributes to the development of AKI.

3.3. PARylation promotes inflammatory response and injury in HK2 cells

We assessed the effect of CIS and H/R stimulation on PARylation in HK2 cells. The CIS-induced increase in KIM-1 expression was attenuated by *PARP1* knockdown, which decreased the PARylation level, and further intensified by overexpression of *PARP1*, which increased the PARylation level (Fig. 3A–F, Supporting Information Fig. S5A–S5E). Additionally, Western blot and real-time PCR analyses showed that reduced PARylation levels alleviated the CIS-induced P65NF-κB phosphorylation and inflammatory cytokine production (Fig. 3B and C, Fig. S5C). In contrast, increased PARylation levels promoted CIS-induced P65NF-κB phosphorylation and inflammatory cytokine production (Fig. 3F and G, Fig. S5E). These findings were confirmed using *in vitro* H/R models. Reduced and elevated PARylation levels prevented and promoted, respectively, H/R-induced KIM-1 accumulation and inflammatory cytokine production (Fig. 3H–J, Fig. S5F–S5J). Furthermore, we used a non-toxic concentration of PDD (1 μmol/L) *in vitro* to increase the level of PARylation (Fig. 3K). PDD treatment markedly increased PAR signalling (Fig. 3L, Fig. S5K) and promoted KIM-1 production and P65 phosphorylation (Fig. 3M and N). To confirm that PARylation itself, rather than PARP1, played a damaging role, we knocked down *PARP1* and increased PARylation with PDD *in vitro*. The result showed that the KIM-1 levels were elevated (Fig. 3O, Fig. S5L). Collectively, these findings suggest that increasing cellular PARylation enhances the inflammatory response and injury in CIS- and H/R-stimulated HK2 cells.

3.4. RACK1 can be PARylated, and PARylation promotes its dimerization

Considering the pivotal role of PARylation in the progression of kidney dysfunction, injury, and inflammation, we investigated the mechanisms by which PARylation affects AKI. Based on the limited information on this process and the potential biological importance of PARylation regulation, we explored proteins that might be PARylated and the mechanisms underlying their regulation in HK2 cells. LC–MS/MS results showed that PARylation of RACK1 in CIS-induced HK2 cells with *PARP1* overexpression exhibited higher coverage and produced more unique peptides (Fig. 4A–C), while RACK1 mediates the process of inflammation[26]. Notably, Western blot analysis revealed that RACK1 expression was significantly increased in CIS-treated HK2 cells and AKI mouse models (Fig. 4D and E). The change in the expression level was partly dependent on the increase or decrease of the PARylation level (Supporting Information Fig. S6A). Co-IP results confirmed an enhanced interaction between PAR and RACK1 in CIS-stimulated HK2 cells, indicating an increase in RACK1 PARylation (Fig. 4F). The kidney lysate was extracted and used for the Co-IP of PAR and RACK1. The results confirmed that the interaction between PAR and RACK1 was similarly enhanced in CIS-induced AKI mouse models compared with that in control mice (Fig. 4G). In addition, the level of PARylated RACK1 decreased or increased with *PARP1* knockdown or PDD, respectively (Fig. 4H–J), and interactions were observed between PARP1 and RACK1 (Fig. 4K).

Previous reports have indicated that different PARP1 variants synthesise PAR with different properties[27]. Among them, a tyrosine-to-serine substitution at amino acid residue 986 of PARP1 (PARP1-Y986S) produces short and moderately hyperbranched PAR, which may produce a stronger PAR-binding capability[28]. Following treatment with wild-type PARP1 or PARP1 Y986S, we performed Co-IP assays. We found that the PAR of PARP1 Y986S displayed increased RACK1 binding (Fig. 4L). Thornton et al.[29] found that spatial and temporal compartmentalisation *via* homo- and hetero-dimerization of RACK1 is important for the transduction of signals. We constructed two differentially labelled *RACK1* plasmids, *FLAG-RACK1* and *MYC-RACK1*, to explore the process of RACK1 dimerization in renal tubular epithelial cells. The Co-IP results showed that the two monomers, FLAG-RACK1 and MYC-RACK1, could bind to each other. After CIS stimulation, dimerization of FLAG-RACK1 and MYC-RACK1 was

with or without RACK1 KD ($n = 3$, one-way ANOVA); (F) Real-time PCR analysis of *TNFA*, *MCP1*, and *IL1B* mRNA levels in H/R-induced cells with or without RACK1 KD ($n = 3$, one-way ANOVA); (G) IF staining of KIM-1 with or without RACK1 KD after PDD treatment in CIS-induced cells. Scale bar = 50 μm; (H) Western blot analysis of KIM-1 with or without RACK1 OE after PARP1 KD in CIS-induced cells ($n = 3$, one-way ANOVA); (I) Real-time PCR analysis of *TNFA*, *MCP1*, and *IL1B* mRNA levels with or without RACK1 OE after PARP1 KD in CIS-induced cells ($n = 3$, one-way ANOVA). Data are mean ± SD; $^*P < 0.05$, $^{**}P < 0.01$, $^{***}P < 0.001$ *vs*. Control/Model.

Please cite this article as: Li Xiangyu et al., PARylation promotes acute kidney injury *via* RACK1 dimerization-mediated HIF-1α degradation, Acta Pharmaceutica Sinica B, https://doi.org/10.1016/j.apsb.2025.07.019

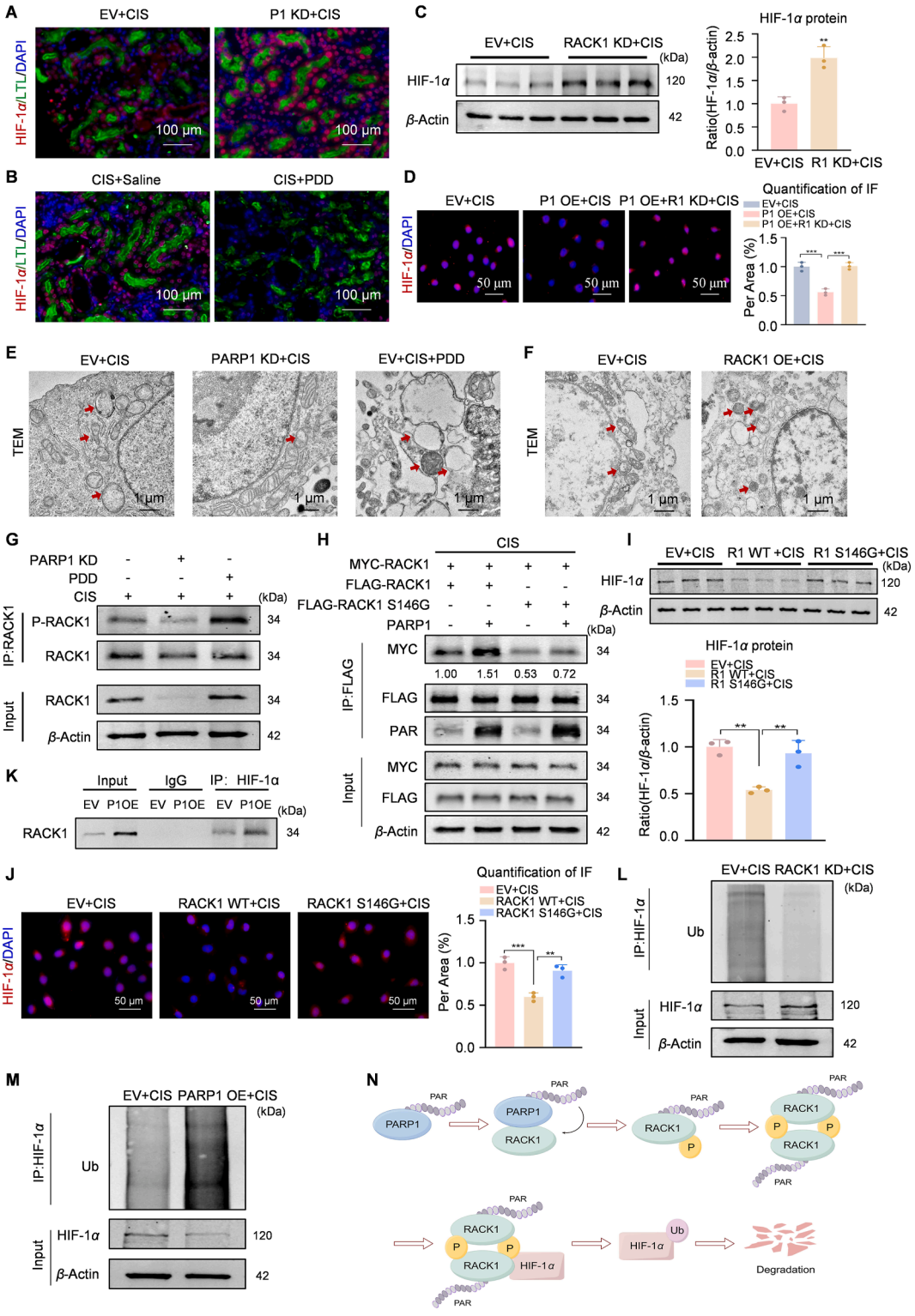

Figure 6 The PARylation of RACK1 enhances its phosphorylation, which subsequently facilitates dimerization and accelerates the ubiquitination-mediated degradation of HIF-1α. (A) Double staining of HIF-1α and LTL in the AAV-EV and AAV-PARP1 KD mice with CIS-induced AKI. Scale bar = 100 μm; (B) Double staining of HIF-1α and LTL in CIS-induced AKI mice with or without PDD. Scale bar = 100 μm; (C) Western blot analysis of HIF-1α in CIS-induced HK2 cells with or without RACK1 KD (n = 3, t-test); (D) IF staining of KIM-1 with or without RACK1 KD after PARP1 OE in CIS-induced cells. Scale bar = 100 μm; (E) Representative transmission electron micrographs (TEMs) of CIS-induced HK2 cells with or without PARP1 KD or PDD. Scale bar = 1 μm; (F) Representative TEMs of CIS-induced HK2 cells with or without RACK1 OE. Scale bar = 1 μm; (G) Co-IP assay indicates the level of RACK1 phosphorylation with or without PARP1 KD or PDD; (H) Co-IP assay indicates the influence of RACK1 S146G on the dimerization of RACK1 in CIS-induced HK2 cells; (I) Western blot

Please cite this article as: Li Xiangyu et al., PARylation promotes acute kidney injury *via* RACK1 dimerization-mediated HIF-1α degradation, Acta Pharmaceutica Sinica B, https://doi.org/10.1016/j.apsb.2025.07.019

enhanced, demonstrating that RACK1 dimerization in the model was essential for gene regulation (Fig. 4M). Additionally, *PARP1* overexpression and PDD treatment to increase PARylation levels significantly promoted the dimerization of RACK1, suggesting that PARylation in renal tubular epithelial cells might induce damage by affecting RACK1 dimerization (Fig. 4M and N). Collectively, our results suggest that RACK1 is a PAR-binding protein that binds preferentially to short and moderately hyperbranched PAR and that PARylation promotes RACK1 dimerization.

3.5. Disruption of RACK1 attenuates CIS- and H/R-induced cell injury and inflammation

To explore the function of RACK1, we silenced *RACK1* in HK2 cells, which was confirmed by Western blot and real-time PCR (Fig. S6B and S6C). Western blot and IF results showed that *RACK1* silencing reduced the CIS-induced expression of KIM-1 (Fig. 5A and B). Furthermore, *RACK1* knockdown markedly decreased CIS-induced activation of the NF-κB pathway and proinflammatory cytokine production (Fig. 5B and C, Fig. S6D). These findings were further validated in H/R-induced HK2 cells (Fig. 5D−F, Fig. S6E). In addition, *RACK1* silencing alleviated PDD-induced KIM-1 expression, and *RACK1* overexpression restored the KIM-1 expression reduced by *PARP1* knockdown in CIS-treated HK2 cells (Fig. 5G−I, Fig. S6F).

3.6. PARylation of RACK1 promotes its phosphorylation, which in turn promotes dimerization and accelerates the ubiquitination and degradation of HIF-1α

In mouse AKI models, *Parp1* knockdown and decreasing PARylation level increased hypoxia inducible factor-1α (HIF-1α) expression, whereas increasing PARylation level with PDD decreased HIF-1α expression (Fig. 6A and B). Notably, *RACK1* knockdown increased HIF-1α expression (Fig. 6C), and knocking down *RACK1* restored HIF-1α levels reduced by *PARP1* overexpression in CIS-induced HK2 cells (Fig. 6D). In AKI, HIF-1α activation has been repeatedly reported to have a protective effect[30,31], and most studies have highlighted the critical role of HIF-1α in regulating mitochondrial function. HIF-1α modulates metabolic adaptation by downregulating mitochondrial respiration, maintaining mitochondrial redox homeostasis, and facilitating mitophagy[31−33]. Our results showed that CIS-induced mitochondrial damage decreased or increased with changes in PARylation levels (Fig. 6E), and *RACK1* overexpression aggravated CIS-induced mitochondrial damage (Fig. 6F).

Further experiments showed that the RNA level of *HIF1a* was not affected by PARylated RACK1, while the levels of its downstream genes, such as erythropoietin (*EPO*) and vascular endothelial growth factor (*VEGF*), increased significantly after *RACK1* knockdown, indicating that HIF-1α was degraded at the protein level (Supporting Information Fig. S7A−S7C). Previous studies have demonstrated that in HEK293T cells, phosphorylation of RACK1 in the WD4 dimerization domain is required for RACK1 dimerization, which in turn facilitates the ubiquitination and degradation of HIF-1α[34]. Therefore, we hypothesised that PARylation promotes the dimerization of RACK1 by promoting its phosphorylation in HK2 cells. To test this hypothesis, we examined the effects of PARylation on RACK1 phosphorylation levels. Serine 146 (Ser146) is a strong candidate phosphorylation site in the WD4 domain of RACK1[34]. Our Co-IP results suggested that PARylation promoted serine phosphorylation of RACK1 (Fig. 6G). Next, we investigated the effect of serine-to-glycine substitution at amino acid residue 146 (S146G) of RACK1. Remarkably, the binding of FLAG-RACK1 S146G to MYC-RACK1 was significantly reduced compared with that of wild-type FLAG-RACK1 (Fig. 6H). Moreover, RACK1 S146G showed little effect on HIF-1α expression (Fig. 6I and J). Our results further confirmed the interaction between RACK1 and HIF-1α, and showed that *RACK1* knockdown reduced its ubiquitination degradation, whereas increasing the PARylation level promoted its degradation (Fig. 6K−M). The ubiquitination and proteasome degradation of HIF-1α after hydroxylation by prolyl hydroxylase is the main way of HIF-1α degradation[35]. DMOG is a competitive inhibitor of HIF-1α prolyl hydroxylase (HIF-PH) that can penetrate cells. We treated *PARP1* overexpressed cells in the model with DMOG and found that HIF-1α ubiquitination levels were significantly reduced, indicating that HIF-1α degradation might be partially prolyl hydroxylase-dependent (Fig. S7D). In addition, as members of the HIF-α family, HIF-1α and HIF-2α share structural similarities and several common target genes, but they have different physiological and pathological functions[36]. In this context, is HIF-2α expression regulated by PARylation? Our results suggested that PARylation did not affect HIF-2α expression levels in CIS-induced cell damage (Fig. S7E). In general, the PARylation of RACK1 promotes its phosphorylation, which in turn promotes dimerization and accelerates the ubiquitination and degradation of HIF-1α (Fig. 6N).

3.7. PARP1 proteolysis-targeting chimera (PROTAC) ***A19*** confers renal protection both in vitro and in vivo

Our findings underscore the critical role of PARylation in the pathogenesis and progression of AKI and highlight its significant potential as a target for preventive and therapeutic strategies. PARP1 is the primary enzyme responsible for synthesizing PAR, so inhibiting PARP1 is the most efficient way to decrease PARylation. Subsequently, we aimed to develop targeted therapeutic agents. The key limitations of PARP1 inhibitors are resistance and limited selectivity[37−40]. However, PROTACs can address drug resistance by selectively degrading PARP1 instead of merely inhibiting its activity, thereby offering enhanced targeting and specificity within the cell.

analysis of HIF-1α in CIS-induced HK2 cells with wild RACK1 or RACK1 S146G ($n = 3$, one-way ANOVA); (J) IF staining of HIF-1α in CIS-induced HK2 cells with wild RACK1 or RACK1 S146G. Scale bar = 100 μm; (K) Co-IP assay indicates the interactions of RACK1 and HIF-1α in PARP1 OE cells; (L) Applied with or without RACK1 KD in CIS-induced HK2 cells. HIF-1α was isolated by IP, and HIF-1α ubiquitination levels were assessed with ubiquitin antibodies; (M) Applied with or without PARP1 OE in CIS-induced HK2 cells. HIF-1α was isolated by IP, and HIF-1α ubiquitination levels were assessed with ubiquitin antibodies; (N) Diagram depicting PARylation promotes the dimerization of RACK1 by promoting its phosphorylation and accelerates the ubiquitination degradation of HIF-1α (by Figdraw 2.0). Data are mean ± SD; $^{*}P < 0.05$, $^{**}P < 0.01$, $^{***}P < 0.001$ *vs*. Control/Model.

Please cite this article as: Li Xiangyu et al., PARylation promotes acute kidney injury *via* RACK1 dimerization-mediated HIF-1α degradation, Acta Pharmaceutica Sinica B, https://doi.org/10.1016/j.apsb.2025.07.019

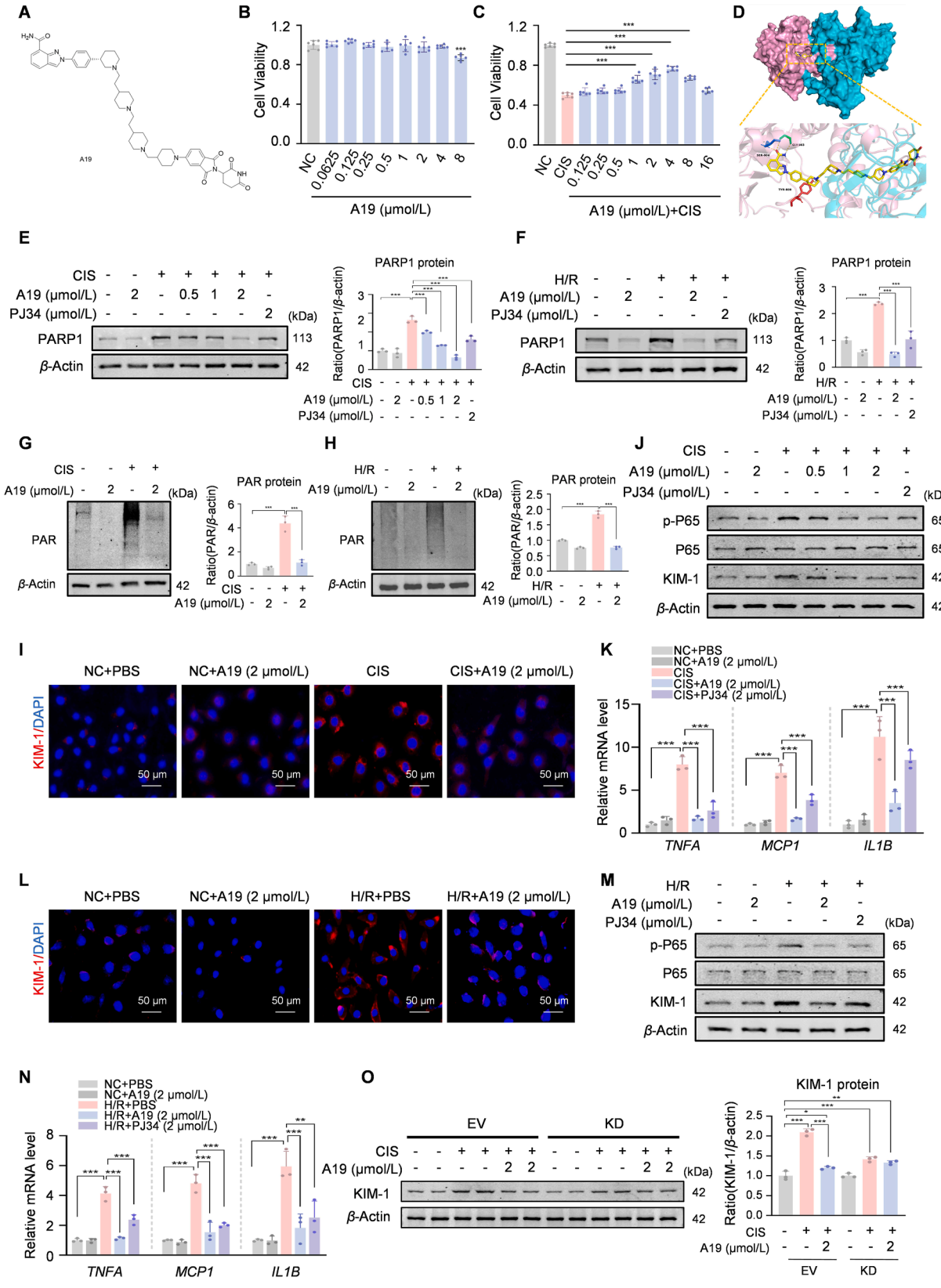

Figure 7 Novel PROTAC **A19** alleviates CIS- and H/R-induced cell injury and inflammation by degrading PARP1 and reducing PARylation levels *in vitro*. (A) Structural formula of **A19**; (B) Cell viability assay of HK2 cells treated with different concentrations of **A19**; (C) **A19** restored the cell viability in CIS-induced HK2 cells; (D) Computational simulation of molecular docking between PARP1 and **A19**; (E) Western blot analysis of PARP1 under the influence of 0.5, 1, and 2 μmol/L **A19** and 2 μmol/L PJ34 in CIS-induced HK2 cells ($n = 3$, one-way ANOVA); (F) Western blot analysis of PARP1 under the influence of 2 μmol/L **A19** and 2 μmol/L PJ34 in H/R-induced HK2 cells ($n = 3$, one-way ANOVA);

Please cite this article as: Li Xiangyu et al., PARylation promotes acute kidney injury *via* RACK1 dimerization-mediated HIF-1α degradation, Acta Pharmaceutica Sinica B, https://doi.org/10.1016/j.apsb.2025.07.019

For this purpose, we identified **A19** as a potent PARP1-targeting PROTAC, which is a class of compounds capable of degrading target proteins by harnessing the ubiquitin−proteasome system (UPS; Fig. 7A, Scheme S1, Fig. S1). We performed the MTT assay to evaluate the effect of **A19** on cell viability. At concentrations exceeding 8 μmol/L, **A19** affected the growth of HK2 cells (Fig. 7B). Subsequently, we determined the effect of **A19** on CIS-induced cell injury. At 0.5, 1, and 2 μmol/L, **A19** restored the viability of CIS-treated HK2 cells in a concentration-dependent manner (Fig. 7C). Notably, the effective degradation of PARP1 by PROTAC **A19** relies on the formation of favourable ternary complexes as a key requirement. The simulated structure of the PARP1−**A19**−cereblon ternary complex strongly supported the beneficial role of **A19** in PARP1 degradation (Fig. 7D).

Western blot verified that **A19** effectively degraded PARP1 and reduced PAR in cell models induced by CIS and H/R (Fig. 7E−H). NAD^+ is a PARylation substrate, and reducing the PARylation level with **A19** could effectively restore the NAD^+ level in CIS-induced HK2 cells (Supporting Information Fig. S8A). Additionally, we discovered that the administration of **A19** before CIS-induced cellular insult led to a dose-dependent reduction in KIM-1, P65 phosphorylation, and proinflammatory cytokines production (Fig. 7I−K, Fig. S8B and S8C). Compared with the well-known PARP1 inhibitor PJ34, **A19** showed better protection. Consistent with these observations, we found that **A19** ameliorated cellular injury and inflammation in an *in vitro* H/R-induced cell injury model, thereby reinforcing the potential of the compound as a broad-spectrum intervention against renal injury (Fig. 7L−N, Fig. S8D and S8E). Moreover, in CIS-treated *PARP1* knockdown cells, **A19** did not further alleviate cell injury compared with that in untreated **A19** cells (Fig. 7O, Fig. S8F). More importantly, **A19** did not degrade PARP2, PARP5a, and PARP5b, which are other PARylation-related enzymes (Fig. S8G). These results indicate that **A19** mainly targets PARP1 to mitigate damage.

We initiated a preliminary pharmacological investigation by establishing drug concentration gradients in murine models (Fig. 8A). Accordingly, male C57BL/6J mice were pre-treated with the saline, **A19** (2.5, 5, or 10 mg/kg body weight), or PJ34 (10 mg/kg body weight), followed by an intraperitoneal injection of CIS (20 mg/kg body weight) after 12 h. Western blot analysis verified the effective concentrations for PARP1 degradation (Fig. 8B). The **A19**-treated group exhibited a dose-dependent decrease in serum CRE and BUN compared with the CIS model group (Fig. 8C and D), along with a significant decrease in the levels of KIM-1, renal glycogen deposition, and tubular dilation (Fig. 8E−G, Supporting Information Fig. S9A−S9D). P65 phosphorylation and the production of proinflammatory cytokines were significantly reduced (Fig. 8E, Fig. S9A and S9E). The same preventive effect was observed in I/R-induced AKI models (Fig. 8H−J, Fig. S9F). **A19** exerted better nephron-protective effects than PJ34. Furthermore, the histological examination of vital organs, including the heart, liver, spleen, and lungs, revealed no discernible detrimental effects, confirming the lack of significant toxic side effects associated with **A19** administration within the tested dosage range (Fig. S9G). Collectively, our results demonstrate that **A19**, a novel PARP1 degrader, exhibits significant protective effects against kidney injury and inflammation in different AKI models by effectively targeting PAR.

4. Discussion

PTMs can influence all aspects of protein function, and their regulation of protein stability is essential for maintaining cellular homeostasis and preventing disease[8]. PARylation is a recently discovered PTM that plays a critical role in physiological processes and disease development. Investigating the dynamics and spectrum of PARylation and its functional significance in diseases could pave the way for the development of effective intervention, prevention, and treatment strategies. Nevertheless, limited research has concentrated on the role of PARylation in kidney diseases, particularly in AKI. In the present study, we linked PARylation to AKI. PARP1, the primary enzyme responsible for PAR production, showed significantly increased expression in TECs in response to AKI. This upregulation occurred *via* an H3K4me3-dependent mechanism. PARylation exacerbated renal inflammation and injury by PARylating RACK1, which facilitated its dimerization and accelerated the degradation of HIF-1α through ubiquitination. Treatment with **A19**, a PARP1 PROTAC, or AAV9-mediated PARP1 silencing conferred protection against renal injury and inflammation. In contrast, enhanced PARylation following PDD treatment resulted in exacerbated renal inflammation and injury. Collectively, these results indicate that PARylation is a promising therapeutic target for AKI.

We observed a significant increase in PARP1 and PARylation levels, particularly in renal tubular epithelial cells in the kidneys of AKI mice. Histone PTMs function as epigenetic codes, in which individual marks convey their message[41]. One of the best-characterised histone PTMs associated with transcription is H3K4me3, which facilitates the recruitment of transcriptional machinery, thereby promoting transcription[42]. This insight led us to explore the potential epigenetic reconfiguration of PARP1. As expected, our integrated approach, combining bioinformatics prediction with experimental validation, revealed significant methylation modifications on histone H3 associated with PARP1. In AKI, the marked upregulation of PARP1 was hypothesised to be largely driven by H3K4me3 modifications. Subsequently, PARP1 generated more PAR chains, resulting in elevated PARylation levels. This epigenetic event may serve as a critical mechanism underlying increased PARylation observed in renal

(G, H) Western blot analysis of PAR under the influence of 2 μmol/L **A19** in CIS and H/R-induced HK2 cells ($n = 3$, one-way ANOVA); (I) IF staining of KIM-1 in CIS-induced cells after treatment with 2 μmol/L **A19**. Scale bar = 50 μm; (J) Western blot analysis of KIM-1, p-P65, and P65 in CIS-induced HK2 cells after pre-treatment with 0.5, 1, and 2 μmol/L **A19** and 2 μmol/L PJ34 ($n = 3$); (K) Real-time PCR analysis of *TNFA*, *MCP1*, and *IL1B* mRNA levels in CIS-induced cells after treatment with 2 μmol/L **A19** and 2 μmol/L PJ34 ($n = 3$, one-way ANOVA); (L) IF staining of KIM-1 in H/R-induced cells after treatment with 2 μmol/L **A19**. Scale bar = 50 μm; (M) Western blot analysis of KIM-1, p-P65, and P65 in H/R-induced HK2 cells after pre-treatment with 2 μmol/L **A19** and 2 μmol/L PJ34 ($n = 3$); (N) Real-time PCR analysis of *TNFA*, *MCP1*, and *IL1B* mRNA levels in H/R-induced cells after treatment with 2 μmol/L **A19** and 2 μmol/L PJ34 ($n = 3$, one-way ANOVA); (O) Western blot analysis of KIM-1 ($n = 3$, one-way ANOVA). **A19** does not further alleviate injury when PARP1 is silenced. Data are mean ± SD; $^*P < 0.05$, $^{**}P < 0.01$, $^{***}P < 0.001$ *vs*. Control/Model.

Please cite this article as: Li Xiangyu et al., PARylation promotes acute kidney injury *via* RACK1 dimerization-mediated HIF-1α degradation, Acta Pharmaceutica Sinica B, https://doi.org/10.1016/j.apsb.2025.07.019

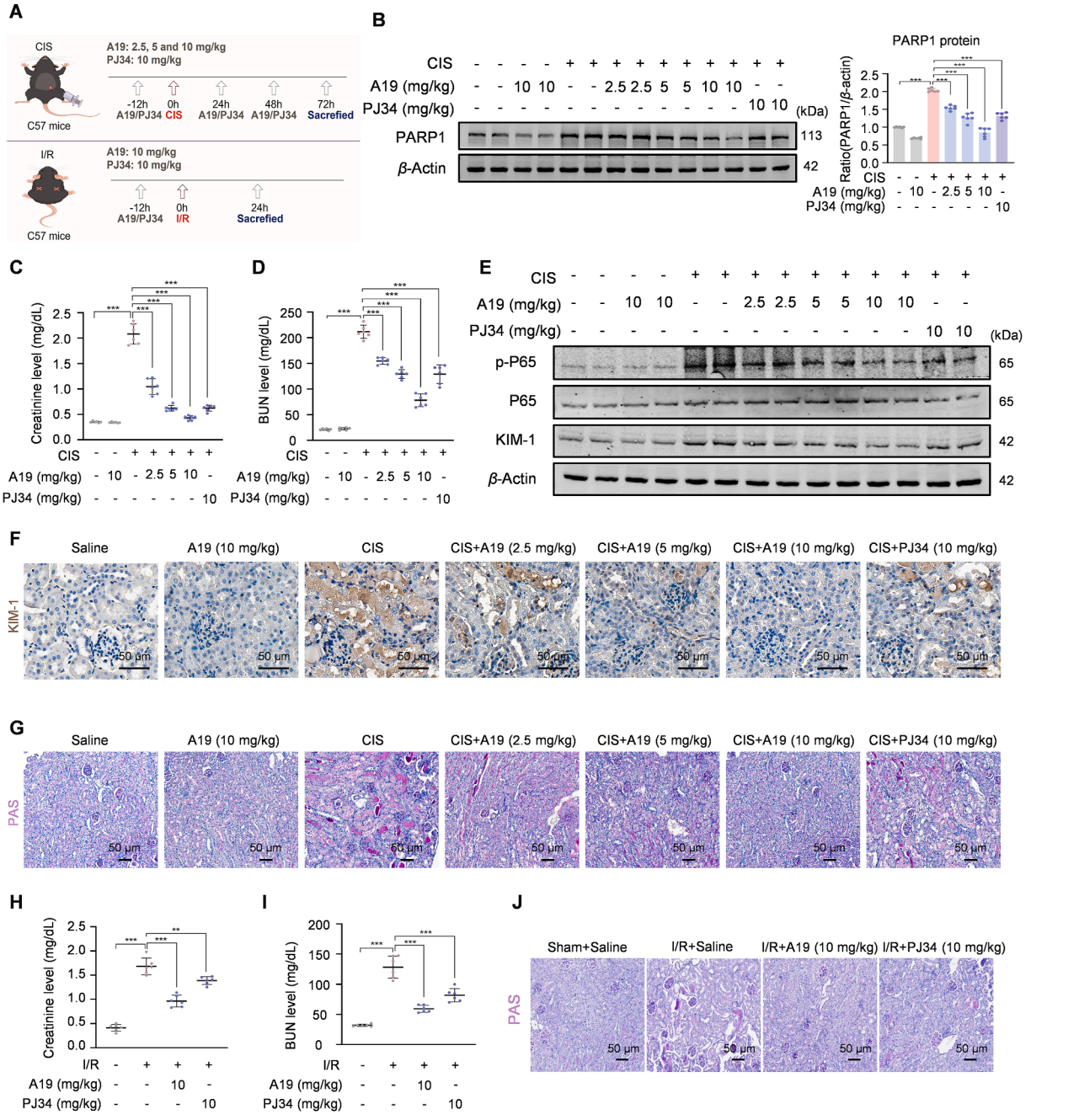

Figure 8 Novel PROTAC **A19** mitigates CIS- and I/R-induced kidney injury and inflammation by degrading PARP1 and reducing PARylation levels *in vivo*. (A) Schematic diagram of the preventive treatment strategy (by Figdraw 2.0); (B) Western blot analysis of PARP1 in CIS-induced AKI mice treated with 2.5, 5, and 10 mg/kg **A19** and 10 mg/kg PJ34 ($n = 6$, one-way ANOVA); (C, D) Serum CRE and BUN in CIS-induced AKI mice treated with 2.5, 5, and 10 mg/kg **A19** and 10 mg/kg PJ34 ($n = 6$, one-way ANOVA); (E) Western blot analysis of KIM-1, p-P65, and P65 in CIS-induced AKI mice treated with 2.5, 5, and 10 mg/kg **A19** and 10 mg/kg PJ34 ($n = 6$); (F) IHC staining of KIM-1 in CIS-induced AKI mice treated with 2.5, 5, and 10 mg/kg **A19** and 10 mg/kg PJ34. Scale bar = 50 μm; (G) PAS staining in CIS-induced AKI mice treated with 2.5, 5, and 10 mg/kg **A19** and 10 mg/kg PJ34. Scale bar = 50 μm; (H, I) Serum CRE and BUN in I/R-induced AKI mice treated with 10 mg/kg **A19** and 10 mg/kg PJ34 ($n = 6$, one-way ANOVA); (J) PAS staining in I/R-induced AKI mice treated with 10 mg/kg **A19** and 10 mg/kg PJ34. Scale bar = 50 μm. Data are mean ± SD; $^{*}P < 0.05$, $^{**}P < 0.01$, $^{***}P < 0.001$ *vs.* Control/Model.

Please cite this article as: Li Xiangyu et al., PARylation promotes acute kidney injury *via* RACK1 dimerization-mediated HIF-1α degradation, Acta Pharmaceutica Sinica B, https://doi.org/10.1016/j.apsb.2025.07.019

pathophysiology, providing a novel perspective on PARylation regulation in AKI. However, the specific epigenetic mechanisms that drive the upregulation and dysregulation of PARylation in AKI remain unclear and warrant further investigation.

Numerous studies have demonstrated that PARP1 activation contributes to kidney injury induced by CIS or I/R[43,44]. Our previous findings suggested that the disruption of PARP1 attenuates CIS- and H/R-induced cell injury and inflammation[19]. PARP1 catalyses the polymerisation of ADP-ribose units to form PAR chains, which modify various target proteins. These modifications regulate essential cellular processes, including DNA damage repair, inflammation, metabolism, and cell death[12,40,45]. Schwarz et al.[46] highlighted the critical role of covalent protein PARylation in coordinating the molecular processes related to dynamic DNA methylation. This interplay between PARylation and DNA methylation suggests a complex mechanism by which PARP1-mediated modifications influence gene expression and epigenetic regulation. Chen et al.[47] elucidated that PARP1-catalysed PARylation of YY1 influences endoplasmic reticulum stress in granulosa cells, affecting primordial follicle activation, which highlighted the importance of PARylation in regulating cellular stress responses and reproductive processes. In the murine central nervous system, Wang et al.[11] suggested that PARP1-mediated PARylation activity could serve as a potential therapeutic target for promoting oligodendrocyte precursor cell differentiation and remyelination in neurological disorders. Therefore, we hypothesised that PARylation played a critical role in renal injury and inflammation. We found that PARylation promoted cell damage and inflammation in HK2 cells. Additionally, we confirmed the importance of PARylation in renal injury using AAV9-packaged *Parp1* knockdown plasmid in different AKI models. Besides, the use of the PARG inhibitor PDD to increase PARylation levels further supported our hypothesis. Collectively, these results suggest that PARylation drives kidney damage and inflammation.

In addition, the exact mechanism underlying PARylation in renal tubular cells during kidney injury is not fully understood. In our study, LC−MS/MS demonstrated a strong binding affinity between PAR and RACK1 in CIS-treated *PARP1* overexpressing HK2 cells. Co-IP results further confirmed that the degree of RACK1 PARylation was increased in the CIS-induced models. Additionally, *PARP1* knockdown reduced the PARylation level of RACK1, whereas the use of PDD increased the PARylation level of RACK1. As a highly conserved member of the tryptophan−aspartic acid (WD) repeat protein family, RACK1 is recognised as a multifunctional scaffold protein that plays a pivotal role in various biological processes, including proliferation, cell migration, apoptosis, and development[48]. PARylation facilitates the dimerization of RACK1, a process crucial for the transmission of signals[29]. We explored the functional role of RACK1 in kidney injury and inflammation. In kidney diseases, RACK1 plays a crucial role in the progression of fibrosis[49,50]. In this study, we demonstrated that *RACK1* knockdown mitigated both kidney injury and inflammation. The use of PDD increased the level of RACK1 PARylation, thereby exacerbating the damage, whereas *RACK1* knockdown reversed this damage. Thus, PARylation may promote kidney injury *via* RACK1-dependent mechanisms.

Previous studies have shown that PARylation is associated with various stress responses and ubiquitination-related processes. Sun et al.[51] discovered that PARylation attracts the deubiquitylating enzyme ubiquitin-specific protease 7, which then reverses the ubiquitination of PARylated topoisomerase I DNA−protein crosslinks. In addition, Wu et al.[52] identified PARylated hexokinase-I (HK-I) as a novel substrate of the E3 ligase ring finger protein 146. They found that crocetin interacts with HK-I to inhibit ring finger protein 146-mediated degradation of HK-I during the later stages of parthanatos, thereby preventing mitochondrial dysfunction and DNA damage. In the present study, we revealed the crosstalk between PARylation and phosphorylation, PARylation promoted the phosphorylation of RACK1 at serine, and phosphorylation at Ser^{146} subsequently promoted RACK1 dimerization. Therefore, we hypothesised that PARylation facilitates RACK1 dimerization by promoting RACK1 Ser^{146} phosphorylation. RACK1 dimerization is crucial for its functional activity, as it can promote the ubiquitination-mediated degradation of HIF-1α[34]. HIF-1α has been reported to exert a protective effect against the progression of AKI, primarily by modulating inflammation, immune response, oxidative stress, and other related mechanisms[31,53]. The present study confirms that PARylated RACK1 promotes the Ser^{146} phosphorylation, thereby promoting the degradation of HIF-1α in CIS-induced HK2 cells, which aggravates mitochondrial damage.

Despite the promising initial response to PARPi therapy, with significant improvements in both progression-free and overall survival, the majority of patients ultimately develop resistance over time. Various mechanisms of PARPi resistance have been identified, including alterations in drug metabolism (*e.g.*, enhanced drug efflux), modulation of PARP activity, and adaptation of DNA repair pathways[54]. Targeted protein degradation (TPD) is gaining significant attention because of its potential to therapeutically modulate proteins that are challenging to target using traditional small molecules. A major class of molecules that can facilitate the modulation of such proteins through TPD is PROTACs, which are designed to promote protein degradation[55−57]. The core concept of PROTAC is that this bifunctional molecule simultaneously binds to a protein of interest (POI) at one end and an E3 ligase at the other, forming a ternary complex that recruits the cellular UPS to facilitate the proteasomal degradation of the POI[58,59]. Unlike with small-molecule inhibitors, binding in this process does not need to be as tight or long-lasting, as it does not rely on sustained occupancy. Meanwhile, since PROTACs require only two binding ligands to bring the POI into proximity with E3 ligases, this approach has the potential to target a wide range of proteins, including those previously considered "undruggable"[60]. Moreover, several PROTACs are anticipated to overcome mutation-induced resistance, which frequently affects their small-molecule inhibitor counterparts.

A significant breakthrough in the current study was the development of a novel PROTAC that utilised the UPS to facilitate ubiquitination-mediated degradation of PARP1, effectively reducing PARylation levels. We meticulously engineered **A19**, a potent PARP1 degrader, which, at a dose of 10 mg/kg, effectively sustained the degradation of PARP1 in renal tissues, serving as a therapeutic intervention for AKI. This intervention balanced PARylation levels, significantly alleviating kidney injury and inflammation and providing innovative therapeutic insights regarding the prevention and treatment of AKI. Nevertheless, the inactivation of PARG and ADP-ribosylhydrolase 3 could restore and enhance PAR signalling. Further studies are needed to evaluate the efficacy of targeting PARG and ADP-ribosylhydrolase 3 as potential therapeutic strategies for improving AKI, as well as to explore additional avenues for intervention in this clinically important condition.

Please cite this article as: Li Xiangyu et al., PARylation promotes acute kidney injury *via* RACK1 dimerization-mediated HIF-1α degradation, Acta Pharmaceutica Sinica B, https://doi.org/10.1016/j.apsb.2025.07.019

5. Conclusions

Collectively, our results showed that PARP1 and the level of PARylation are markedly upregulated in tubular epithelial cells in an H3K4me3-dependent manner in AKI. PARylation predominantly occurs on RACK1, and the PARylation of RACK1 enhances its phosphorylation, which subsequently facilitates RACK1 dimerization. This dimerization accelerates the degradation of HIF-1α, thereby exacerbating the progression of acute kidney injury. Concurrently, the development of PARP1-specific PROTACs presents a promising therapeutic approach for the targeted modulation of PARylation in the treatment of AKI.

Acknowledgements

This work was supported by the National Natural Science Foundation of China (No. 82270738), National Key R&D Program (2022YFC2502503, China) and Scientific Research Project of Education Department of Anhui Province (No. 2023AH053398, China).

Author contributions

Xiaoming Meng, Jutao Yu and Xiangyu Li supervised the research, designed the experiments, and wrote the paper. Xiangyu Li and Xiaoyu Shen designed the study and analyzed the data. Mingfei Wu and Xinfei Mao performed drug design and synthesis. Xiangyu Li, Yuqing Wang, Yuhang Dong and Shuai Sun performed part of the cellular experiments and histological analysis. Xiangyu Li, Mengmeng Zhang, Jie Wei, Jianan Wang, Chao Li and Minglu Ji conducted part of the animal experiments. Xiangyu Li, Xiaowei Hu and Xinyu Chen interpreted the results. Juan Jin, Jiagen Wen and Yujie Liu provided a series of experimental instructions and help. All authors have revised and approved the final manuscript.

Conflicts of interest

The authors declare no conflicts of interest.

Appendix A. Supporting information

Supporting information to this article can be found online at https://doi.org/10.1016/j.apsb.2025.07.019.

References

1. Legrand M, Clark AT, Neyra JA, Ostermann M. Acute kidney injury in patients with burns. *Nat Rev Nephrol* 2024;**20**:188−200.
2. Yu P, Gu T, Rao Y, Liang W, Zhang X, Jiang H, et al. A novel marine-derived anti-acute kidney injury agent targeting peroxiredoxin 1 and its nanodelivery strategy based on ADME optimization. *Acta Pharm Sin B* 2024;**14**:3232−50.
3. Kellum JA, Romagnani P, Ashuntantang G, Ronco C, Zarbock A, Anders HJ. Acute kidney injury. *Nat Rev Dis Primers* 2021;**7**:52.
4. Ronco C, Bellomo R, Kellum JA. Acute kidney injury. *Lancet* 2019; **394**:1949−64.
5. Ma T, Li H, Liu H, Peng Y, Lin T, Deng Z, et al. Neat 1 promotes acute kidney injury to chronic kidney disease by facilitating tubular epithelial cells apoptosis *via* sequestering miR-129-5p. *Mol Ther* 2022;**30**:3313−32.
6. Li ZL, Li XY, Zhou Y, Wang B, Lv LL, Liu BC. Renal tubular epithelial cells response to injury in acute kidney injury. *eBioMedicine* 2024;**107**:105294.
7. Kumar S. Cellular and molecular pathways of renal repair after acute kidney injury. *Kidney Int* 2018;**93**:27−40.
8. Lee JM, Hammarén HM, Savitski MM, Baek SH. Control of protein stability by post-translational modifications. *Nat Commun* 2023;**14**: 201.
9. Kim D-S, Challa S, Jones A, Kraus WL. PARPs and ADP-ribosylation in RNA biology: from RNA expression and processing to protein translation and proteostasis. *Genes Dev* 2020;**34**: 302−20.
10. Kamaletdinova T, Fanaei-Kahrani Z, Wang ZQ. The enigmatic function of PARP1: from PARylation activity to PAR readers. *Cells* 2019; **8**:1625.
11. Wang Y, Zhang Y, Zhang S, Kim B, Hull VL, Xu J, et al. PARP1-mediated PARylation activity is essential for oligodendroglial differentiation and CNS myelination. *Cell Rep* 2021;**37**:109695.
12. Alemasova EE, Lavrik OI. Poly(ADP-ribosyl)ation by PARP1: reaction mechanism and regulatory proteins. *Nucleic Acids Res* 2019;**47**: 3811−27.
13. Tufan AB, Lazarow K, Kolesnichenko M, Sporbert A, Von Kries JP, Scheidereit C. TSG101 associates with PARP1 and is essential for PARylation and DNA damage-induced NF-κB activation. *EMBO J* 2022;**41**:e110372.
14. Zhang XN, Lam AT, Cheng Q, Courouble VV, Strutzenberg TS, Li J, et al. Discovery of an NAD^+ analogue with enhanced specificity for PARP1. *Chem Sci* 2022;**13**:1982−91.
15. Wu S, Li X, Gao F, De Groot JF, Koul D, Yung WKA. PARP-mediated PARylation of MGMT is critical to promote repair of temozolomide-induced O^6-methylguanine DNA damage in glioblastoma. *Neuro Oncol* 2021;**23**:920−31.
16. Bolderson E, Burgess JT, Li J, Gandhi NS, Boucher D, Croft LV, et al. Barrier-to-autointegration factor 1 (Banf1) regulates poly [ADP-ribose] polymerase 1 (PARP1) activity following oxidative DNA damage. *Nat Commun* 2019;**10**:5501.
17. Yang Q, Ren G, Wei B, Jin J, Huang XR, Shao W, et al. Conditional knockout of TGF-βRII/Smad2 signals protects against acute renal injury by alleviating cell necroptosis, apoptosis and inflammation. *Theranostics* 2019;**9**:8277−93.
18. Li C, Ma Q, Liu X, Li H, Yu M, Xie S, et al. Genetic and pharmacological inhibition of GRPR protects against acute kidney injury *via* attenuating renal inflammation and necroptosis. *Mol Ther* 2023;**31**: 2734−54.
19. Yu J, Hu X, Yang Q, Shan R, Zhang Y, Dong Z, et al. Insulin-like growth factor binding protein 7 promotes acute kidney injury by alleviating poly ADP ribose polymerase 1 degradation. *Kidney Int* 2022;**102**:828−44.
20. Wang J, Wang F, Ke J, Li Z, Xu C, Yang Q, et al. Inhibition of *METTL3* attenuates renal injury and inflammation by alleviating *TAB3* m6A modifications *via* IGF2BP2-dependent mechanisms. *Sci Transl Med* 2022;**14**:eabk2709.
21. Wang J, Liu M, Wang F, Wei B, Yang Q, Cai Y, et al. RIPK1 inhibitor Cpd-71 attenuates renal dysfunction in cisplatin-treated mice *via* attenuating necroptosis, inflammation and oxidative stress. *Clin Sci* 2019;**133**:1609−27.
22. Yu JT, Hu XW, Chen HY, Yang Q, Li HD, Dong YH, et al. DNA methylation of FTO promotes renal inflammation by enhancing m6A of PPAR-α in alcohol-induced kidney injury. *Pharmacol Res* 2021; **163**:105286.
23. Wang JN, Yang Q, Yang C, Cai YT, Xing T, Gao L, et al. Smad3 promotes AKI sensitivity in diabetic mice *via* interaction with p53 and induction of NOX4-dependent ROS production. *Redox Biol* 2020;**32**: 101479.
24. Dixon EE, Wu H, Muto Y, Wilson PC, Humphreys BD. Spatially resolved transcriptomic analysis of acute kidney injury in a female murine model. *JASN* 2022;**33**:279−89.

25. Shimoda H, Doi S, Nakashima A, Sasaki K, Doi T, Masaki T. Inhibition of the H3K4 methyltransferase MLL1/WDR5 complex attenuates renal senescence in ischemia reperfusion mice by reduction of p16. *Kidney Int* 2019;**96**:1162−75.
26. Yao F, Long LY, Deng YZ, Feng YY, Ying GY, Bao WD, et al. RACK1 modulates NF-κB activation by interfering with the interaction between TRAF2 and the IKK complex. *Cell Res* 2014;**24**:359−71.
27. Aberle L, Krüger A, Reber JM, Lippmann M, Hufnagel M, Schmalz M, et al. PARP1 catalytic variants reveal branching and chain length-specific functions of poly(ADP-ribose) in cellular physiology and stress response. *Nucleic Acids Res* 2020;**48**:10015−33.
28. Fu X, Zhang J, Sun K, Zhang M, Wang S, Yuan M, et al. Poly (ADP-ribose) polymerase 1 promotes HuR/ELAVL1 cytoplasmic localization and inflammatory gene expression by regulating p38 MAPK activity. *Cell Mol Life Sci* 2024;**81**:253.
29. Thornton C, Tang K-C, Phamluong K, Luong K, Vagts A, Nikanjam D, et al. Spatial and temporal regulation of RACK1 function and *N*-methyl-D-aspartate receptor activity through WD40 motif-mediated dimerization. *J Biol Chem* 2004;**279**:31357−64.
30. Rajendran G, Schonfeld MP, Tiwari R, Huang S, Torosyan R, Fields T, et al. Inhibition of endothelial PHD2 suppresses post-ischemic kidney inflammation through hypoxia-inducible factor-1. *JASN* 2020;**31**:501−16.
31. Li W, Xiang Z, Xing Y, Li S, Shi S. Mitochondria bridge HIF signaling and ferroptosis blockage in acute kidney injury. *Cell Death Dis* 2022;**13**:308.
32. Li HS, Zhou YN, Li L, Li SF, Long D, Chen XL, et al. HIF-1α protects against oxidative stress by directly targeting mitochondria. *Redox Biol* 2019;**25**:101109.
33. Jiang N, Zhao H, Han Y, Li L, Xiong S, Zeng L, et al. HIF-1α ameliorates tubular injury in diabetic nephropathy *via* HO-1-mediated control of mitochondrial dynamics. *Cell Prolif* 2020;**53**:e12909.
34. Liu YV, Hubbi ME, Pan F, McDonald KR, Mansharamani M, Cole RN, et al. Calcineurin promotes hypoxia-inducible factor 1α expression by dephosphorylating RACK1 and blocking RACK1 dimerization. *J Biol Chem* 2007;**282**:37064−73.
35. Schödel J, Ratcliffe PJ. Mechanisms of hypoxia signalling: new implications for nephrology. *Nat Rev Nephrol* 2019;**15**:641−59.
36. Jeelani I, Moon JS, Da Cunha FF, Nasamran CA, Jeon S, Zhang X, et al. HIF-2α drives hepatic Kupffer cell death and proinflammatory recruited macrophage activation in nonalcoholic steatohepatitis. *Sci Transl Med* 2024;**16**:eadi0284.
37. Mateo J, Lord CJ, Serra V, Tutt A, Balmaña J, Castroviejo-Bermejo M, et al. A decade of clinical development of PARP inhibitors in perspective. *Ann Oncol* 2019;**30**:1437−47.
38. Curtin NJ, Szabo C. Poly(ADP-ribose) polymerase inhibition: past, present and future. *Nat Rev Drug Discov* 2020;**19**:711−36.
39. Li H, Liu ZY, Wu N, Chen YC, Cheng Q, Wang J. PARP inhibitor resistance: the underlying mechanisms and clinical implications. *Mol Cancer* 2020;**19**:107.
40. Huang D, Kraus WL. The expanding universe of PARP1-mediated molecular and therapeutic mechanisms. *Mol Cell* 2022;**82**:2315−34.
41. Millán-Zambrano G, Burton A, Bannister AJ, Schneider R. Histone post-translational modifications—cause and consequence of genome function. *Nat Rev Genet* 2022;**23**:563−80.
42. Vermeulen M, Mulder KW, Denissov S, Pijnappel WWMP, Van Schaik FMA, Varier RA, et al. Selective anchoring of TFIID to nucleosomes by trimethylation of histone H3 lysine 4. *Cell* 2007;**131**:58−69.
43. Kim MJ, Moon D, Jung S, Lee J, Kim J. Cisplatin nephrotoxicity is induced *via* poly(ADP-ribose) polymerase activation in adult zebrafish and mice. *Am J Physiol Regul Integr Comp Physiol* 2020;**318**:R843−54.
44. Jang HR, Lee K, Jeon J, Kim JR, Lee JE, Kwon GY, et al. Poly (ADP-ribose) polymerase inhibitor treatment as a novel therapy attenuating renal ischemia−reperfusion Injury. *Front Immunol* 2020;**11**:564288.
45. Kang M, Park S, Park SH, Lee HG, Park JH. A double-edged sword: the two faces of PARylation. *IJMS* 2022;**23**:9826.
46. Schwarz SD, Xu J, Gunasekera K, Schürmann D, Vågbø CB, Ferrari E, et al. Covalent PARylation of DNA base excision repair proteins regulates DNA demethylation. *Nat Commun* 2024;**15**:184.
47. Chen W, E Q, Sun B, Zhang P, Li N, Fei S, et al. PARP1-catalyzed PARylation of YY1 mediates endoplasmic reticulum stress in granulosa cells to determine primordial follicle activation. *Cell Death Dis* 2023;**14**:524.
48. Adams DR, Ron D, Kiely PA. RACK1, A multifaceted scaffolding protein: Structure and function. *Cell Commun Signal* 2011;**9**:22.
49. Hou L, Du Y. Neuropilin 1 promotes unilateral ureteral obstruction-induced renal fibrosis *via* RACK1 in renal tubular epithelial cells. *Am J Physiol Renal Physiol* 2023;**325**:F870−84.
50. Bao Q, Wang A, Hong W, Wang Y, Li B, He L, et al. The c-Abl−RACK1−FAK signaling axis promotes renal fibrosis in mice through regulating fibroblast-myofibroblast transition. *Cell Commun Signal* 2024;**22**:247.
51. Sun Y, Chen J, Huang SN, Su YP, Wang W, Agama K, et al. PARylation prevents the proteasomal degradation of topoisomerase I DNA−protein crosslinks and induces their deubiquitylation. *Nat Commun* 2021;**12**:5010.
52. Wu H, Li Y, Zhang Q, Wang H, Xiu W, Xu P, et al. Crocetin antagonizes parthanatos in ischemic stroke *via* inhibiting NOX2 and preserving mitochondrial hexokinase-I. *Cell Death Dis* 2023;**14**:50.
53. Chen Y, Xu J, Shi S, Ma W, Cui W, Yan R, et al. A DNA nanostructure-Hif-1α inducer complex as novel nanotherapy against cisplatin-induced acute kidney injury. *Cell Prolif* 2024;**57**:e13601.
54. Fugger K, Hewitt G, West SC, Boulton SJ. Tackling PARP inhibitor resistance. *Trends Cancer* 2021;**7**:1102−18.
55. Békés M, Langley DR, Crews CM. PROTAC targeted protein degraders: the past is prologue. *Nat Rev Drug Discov* 2022;**21**:181−200.
56. Li X, Song Y. Proteolysis-targeting chimera (PROTAC) for targeted protein degradation and cancer therapy. *J Hematol Oncol* 2020;**13**:50.
57. Huang X, Wu F, Ye J, Wang L, Wang X, Li X, et al. Expanding the horizons of targeted protein degradation: a non-small molecule perspective. *Acta Pharm Sin B* 2024;**14**:2402−27.
58. Jin J, Wu Y, Chen J, Shen Y, Zhang L, Zhang H, et al. The peptide PROTAC modality: a novel strategy for targeted protein ubiquitination. *Theranostics* 2020;**10**:10141−53.
59. Liang T, Wang F, Elhassan RM, Cheng Y, Tang X, Chen W, et al. Targeting histone deacetylases for cancer therapy: trends and challenges. *Acta Pharm Sin B* 2023;**13**:2425−63.
60. Chen Y, Tandon I, Heelan W, Wang Y, Tang W, Hu Q. Proteolysis-targeting chimera (PROTAC) delivery system: advancing protein degraders towards clinical translation. *Chem Soc Rev* 2022;**51**:5330−50.

Please cite this article as: Li Xiangyu et al., PARylation promotes acute kidney injury *via* RACK1 dimerization-mediated HIF-1α degradation, Acta Pharmaceutica Sinica B, https://doi.org/10.1016/j.apsb.2025.07.019